Calibration and Validation of the Urine Nitrification Model

Master Thesis Spring Semester 2015

Author: Gabriel Kämpf

Head: Prof. Dr. Eberhard Morgenroth[1,2]

Supervisors: Dr. Kai M. Udert[2]
                     Dr. Kris Villez[2]

[1] Institute of Environmental Engineering (IfU), Swiss Federal Institiute of Technology Zürich (ETH)

[2] Department of Process Engineering, Swiss Federal Institute of Aquatic Science and Technology (Eawag), Dübendorf, Switzerland

ETH
Eidgenössische Technische Hochschule Zürich
Swiss Federal Institute of Technology Zurich

eawag
aquatic research

IfU
Institut für Umweltingenieurwissenschaften
Institute of Environmental Engineering

Master Thesis Spring Semester 2015

Calibration and Validation of the Urine Nitrification Model

Author: Gabriel Kämpf
                 Luegislandstrasse 507
                 8051 Zürich
                 gabriel.kaempf@gmail.com

Head: Prof. Dr. Eberhard Morgenroth[1,2]

Supervisors: Dr. Kai M. Udert[2]
                 Dr. Kris Villez[2]

[1] Institute of Environmental Engineering (IfU), Swiss Federal Institiute of Technology Zürich (ETH)

[2] Department of Process Engineering, Swiss Federal Institute of Aquatic Science and Technology (Eawag), Dübendorf, Switzerland

Report submitted:
Dübendorf, 11.05.2015

Revised version:
Grosshöchstetten, 31.12.2015

Picture on front page (Gabriel Kämpf): Laboratory nitrification reactors used during this thesis

ETH

Eidgenössische Technische Hochschule Zürich
Swiss Federal Institute of Technology Zurich

Declaration of originality

The signed declaration of originality is a component of every semester paper, Bachelor's thesis, Master's thesis and any other degree paper undertaken during the course of studies, including the respective electronic versions.

Lecturers may also require a declaration of originality for other written papers compiled for their courses.

___

I hereby confirm that I am the sole author of the written work here enclosed and that I have compiled it in my own words. Parts excepted are corrections of form and content by the supervisor.

Title of work (in block letters):

Calibration and Validation of the Urine Nitrification Model

Authored by (in block letters):
For papers written by groups the names of all authors are required.

Name(s):	**First name(s):**
Kämpf	Gabriel

With my signature I confirm that
- I have committed none of the forms of plagiarism described in the 'Citation etiquette' information sheet.
- I have documented all methods, data and processes truthfully.
- I have not manipulated any data.
- I have mentioned all persons who were significant facilitators of the work.

I am aware that the work may be screened electronically for plagiarism.

Place, date	**Signature(s)**
Grosshöchstetten, 31.12.2015 (revised version)	*[signature: G. Kämpf]*

For papers written by groups the names of all authors are required. Their signatures collectively guarantee the entire content of the written paper.

Abstract

In this thesis, the bacterial growth and decay kinetics of urine nitrification was investigated and partly calibrated and validated. The applied model includes a low pH limit of the ammonia oxidizing bacteria (AOB). A sensitivity analysis showed that in case of a serious nitrite accumulation, the parameters of the nitrite oxidizing bacteria (NOB) are more sensitive than the parameters of AOB – except for the maximal growth rate. The calibration and validation experiments were performed in 7-liter completely stirred tank reactors (CSTR) operated with suspended biomass.

As a calibration experiment, a design of four subsequent nitrite pulses was applied. The experiment revealed that NOB are strongly inhibited at concentrations higher than approximately 0.1 mgHNO$_2$/L. This allowed estimating the initial biomass concentration with a maximum uncertainty of 20 and 30% for the lower and the upper boundary, respectively. By means of respirometric measurement of the oxygen uptake rate, the NOB substrate inhibition constant was estimated at 0.112±0.042 mgHNO$_2$/L. Alternatively a maximal NOB growth rate of 7.5±0.8·10^{-5} d^{-1} could be estimated, which is much lower than typical values. Estimating the inhibition constant from activity peaks gives the same value as from respirometry, even with slightly increased accuracy (0.11±0.03 mgHNO$_2$/L). Additionally, there is evidence that the substrate affinity constant needs to be reduced. The decay constant of NOB as well as all parameters of AOB were not identifiable.

Model validation by means of a urine pulse experiment shows that in spite of calibrating the substrate affinity constant, the desired model improvement was not achieved. A reduced inhibition constant was not able to considerably enhance model performance. Further investigations, especially of AOB, and improved parameter estimates will give a better understanding of the real behavior of urine nitrification.

Acknowledgments

Table of Contents

1. Introduction

1.1. Background

This Master thesis is an extension of the VUNA[1] project, which was funded by the Bill & Melinda Gates foundation. The goal of the VUNA is to promote sanitation and nutrient recovery through urine separation. Three major treatment processes for nutrient recovery were proposed: Struvite precipitation, electrolysis and urine nitrification with subsequent distillation. The third process has one major advantage: it allows for recovery of almost all nutrients in one concentrated solution, which can then be used as a fertilizer (Etter, et al., 2015). However, it is also the most complex one; kinetics of urine nitrification is not yet sufficiently understood.

Nitrification is generally assumed to be a two-step process consisting of the transformation of ammonia into nitrous acid (nitritation) by ammonia oxidizing bacteria (AOB) and of nitrous acid into nitrate (nitratation) by nitrite oxidizing bacteria (NOB). In the activated sludge model no. 3 (Gujer, et al., 1999), nitrification is modelled only in one step. This simplification is valid as long as the first process step is rate-limiting, as it is common in municipal wastewater treatment. For urine treatment, however, large substrate concentrations and consequent substrate inhibition can cause that AOB grow faster than NOB. In such cases, severe nitrite accumulation may occur that can lead to complete inhibition and washout of NOB. This necessitates a new start-up of the reactor.

As an important step to predict and avoid such critical situations, a kinetic model including a low pH limit of AOB has been developed by Fumasoli et al. (subm.) and implemented in Matlab (Garbani, 2014). The model is aimed to be applicable regardless the pH, which differs depending on whether there is base addition (complete nitrification, pH between 6 and 7) or not (partial nitrification, pH about 6) (Udert, et al., 2012).

Previous studies have mainly focused on investigating and modelling the biological processes in synthetic urine. Nevertheless, there is still a lack of knowledge about the kinetics in real urine (Etter, et al., 2013). Uhlmann (2014) compared resilience of complete and partial urine nitrification in a moving-bed biofilm reactor (MBBR). As a model approach she used the kinetics and parameter values of Jubany (2007), which includes a sigmoidal pH function for AOB, without a low pH limit. It is the only investigated parameter set that gave reasonable results in both partial and complete nitrification. Nevertheless, the model was not able to predict observed nitrite accumulations following inflow step changes of 30% and 50%.

1.2. Goal and scope of thesis

The aim of the present study was therefore to find an improved parameter set for the biological processes in nitrification of real urine by performing experiments. For this purpose, two urine nitrification reactors were operated at partial nitrification with source-separated urine from the research building (BU) at Eawag.

---

[1] VUNA = Valorisation of Urine Nutrients in Africa; means „harvest" in the isiZulu language

The scope of the thesis was to calibrate and validate the most sensitive AOB and NOB growth and decay parameters in such a way that more reliable predictions of process instabilities due to nitrite accumulation would be possible. An initial sensitivity analysis revealed that the parameters of NOB are more sensitive to nitrite accumulations than the parameters of AOB. Therefore, as a first step to improve the model, the kinetic parameters of NOB were investigated by means of a nitrite pulses experiment. In the calibration step, activity peaks during the batch experiment were used to estimate biomass concentration. Respirometric OUR measurement as used by Jubany (2005) was then applied to find an optimized inhibition constant.

2. Material and methods

2.1. Nitrification model

For this study, the nitrification model 3 as proposed by Fumasoli et al. (subm.) was applied. It includes the growth and decay kinetics of AOB and NOB (section 2.1.1) as well as gas exchange and the acid-base equilibria necessary to model the pH (section 2.1.2). For simulations, NitMod2.3, a model implementation in Matlab, was used (Garbani, 2014).

2.1.1. Kinetics of AOB and NOB

The rate laws of AOB and NOB are both constituted of a growth term ρ_{growth} including a temperature dependent maximal growth rate $\mu^*(T)$ and the biomass concentration X as well as a decay term ρ_{decay} composed of a decay coefficient b^* and X (Jubany, 2007).

Table 1: Process rates of AOB and NOB

Process	Process rate [d^{-1}]
$\rho_{growth,AOB}$	$\begin{cases} 0, & pH < pH_{min} \\ \mu^*_{AOB}(T) \cdot \dfrac{S_{NH_3}}{S_{NH_3} + K_{NH_3,AOB}} \cdot \dfrac{I_{HNO_2,AOB}}{S_{HNO_2} + I_{HNO_2,AOB}} \cdot \left(1 - 10^{K_{pH} \cdot (pH_{min} - pH)}\right) \cdot X_{AOB}, & pH \geq pH_{min} \end{cases}$
$\rho_{decay,NOB}$	$b^*_{AOB}(T) \cdot X_{AOB}$
$\rho_{growth,NOB}$	$\mu^*_{NOB}(T) \cdot \dfrac{S_{HNO_2}}{S_{HNO_2} + K_{HNO_2,NOB} + \dfrac{(S_{HNO_2})^2}{I_{HNO_2,NOB}}} \cdot X_{NOB}$
$\rho_{decay,NOB}$	$b^*_{NOB}(T) \cdot X_{NOB}$

The growth term for AOB further includes a direct pH term as proposed by Fumasoli; below a certain pH limit pH_{min}, AOB activity completely stops (Fumasoli, et al., subm.). Substrate affinity and substrate inhibition of AOB are modelled by means of Monod terms as used by Hellinga et al. (1999), $K_{NH_3,AOB}$ and $I_{HNO_2,AOB}$ being the affinity and inhibition constant of AOB.

Substrate affinity and inhibition of NOB is modelled by using Haldane kinetics as proposed by Hellinga et al. (1999). $K_{HNO_2,NOB}$ and $I_{HNO_2,NOB}$ are the corresponding substrate affinity and subtrate inhibition constant.

The applied parameter values for AOB and NOB are given in Table 2 on the next page. For the growth and decay rates as well as the growth yields, the values were taken from Jubany, et al. (2009). In the case of the substrate affinity and the inhibition constants, the values from Van Hulle, et al. (2007) were applied as it was suggested by Fumasoli, et al. (subm.) for this pH range. The maximal growth rates $\mu^*_{AOB}(T)$ and $\mu^*_{NOB}(T)$ as well as the decay rates $b^*_{AOB}(T)$ and $b^*_{NOB}(T)$ include a temperature dependency. Additionally, the nitrogen fraction and the carbon fraction (i$_N$ and i$_C$, respectively) are given, assuming a biomass composition of $C_5H_7O_2N$.

Due to the different temperature dependency of AOB and NOB, AOB are favored at temperatures above approximately 20°C. Also, the AOB are less strongly inhibited at high HNO$_2$ concentrations than the NOB. In urine nitrification, both conditions are likely to occur, which leads to nitrite accumulation if the AOB

growth is not reduced by some limitation, e.g. substrate limitation which can generally be attained by means of inflow pH control (Udert, et al., 2012). If AOB prevail over NOB, process instabilities or break-down due to severe nitrite accumulations may occur. This may be due to an increase of the nitrogen loading rate or an increase of the temperature (Uhlmann, 2014).

Table 2: Applied kinetic parameters of AOB and NOB

Parameter	Unit	Value	Source
i_n	$molN/gCOD$	0.00625	Assumed biomass compo-
i_c	$molC/gCOD$	0.03125	sition: $C_5H_7O_2N$
$\mu^*_{AOB}(T)$	d^{-1}	$\dfrac{1.28 \cdot 10^{12} \cdot \exp\left(\dfrac{-8183}{273+T}\right)}{1.2545}$	(Jubany, et al., 2009)
$b^*_{AOB}(T)$	d^{-1}	$1.651 \cdot 10^{11} \cdot \exp\left(\dfrac{-8183}{273+T}\right)$	(Jubany, et al., 2009)
Y_{AOB}	$gCOD/molN$	2.52	(Jubany, et al., 2009)
$K_{NH_3,AOB}$	mol/L	$5.357 \cdot 10^{-5}$	(Van Hulle, et al., 2007)
$I_{HNO_2,AOB}$	mol/L	$1.457 \cdot 10^{-4}$	(Van Hulle, et al., 2007)
K_{pH}	$-$	2.1	(Fumasoli, et al., subm.)
pH_{min}	$- (S_{HNO_2} \text{ in } mol/L)$	$\dfrac{S_{HNO_2} + 0.0020088}{0.00037119}$	(Fumasoli, et al., subm.),
$\mu^*_{NOB}(T)$	d^{-1}	$\dfrac{6.69 \cdot 10^7 \cdot \exp\left(\dfrac{-5295}{273+T}\right)}{1.2545}$	(Jubany, et al., 2009)
$b^*_{NOB}(T)$	d^{-1}	$8.626 \cdot 10^6 \cdot \exp\left(\dfrac{-5295}{273+T}\right)$	(Jubany, et al., 2009)
Y_{NOB}	$gCOD/molN$	1.12	(Jubany, et al., 2009)
$K_{NH_3,NOB}$	mol/L	$5.714 \cdot 10^{-7}$	(Jubany, et al., 2009)
$I_{HNO_2,NOB}$	mol/L	$3.214 \cdot 10^{-5}$	(Jubany, et al., 2009)

Oxygen affinity impacts the growth and decay kinetics of the nitrifying species as well; NOB are favored at higher levels of dissolved oxygen (c.p. Jubany (2007)). However, in the model applied in this thesis, no oxygen affinity term is considered.

2.1.2. Acid-base equilibria, complexes and gas exchange

Chemical equilibrium kinetics, complex formation and gas exchange are also taken from Fumasoli et al. (subm.). The chemical equilibria are consequently modelled with back- and forward reactions as proposed by Udert et al. (2003). As an example, the rate expression of the NO_2^-/HNO_2 equilibrium is shown:

$$r_{NO_2^-} = -r_{HNO_2} = k_{eqNH_3} \cdot \left(a_{HNO_2} - a_{NO_2^-} \cdot a_{H^+} \cdot 10^{pK_{NO_2^-}} \right)$$

Due to the high concentrations of some soluble compounds (i) in source-separated urine, the reaction rates have to be calculated by means of ion activities (a_i). These activities are the product of the concentration (c_i) and the activity coefficients (γ_i), which are obtained by means of the ionic strength of the solution (I):

$$a_i = \gamma_i \cdot c_i$$

$$\log(\gamma_i) = -\frac{1}{2} \cdot z_i^2 \cdot \left(\frac{\sqrt{I}}{1 + \sqrt{I}} - 0.2 \cdot I \right)$$

The ionic strength is calculated as a function of the valence (z_i) of each soluble compound (i):

$$I = \frac{1}{2} \cdot \sum_i z_i^2 \cdot c_i$$

All model parameter values related to acid-base equilibria, complex formation and gas exchange can be found in appendix A.1. They were not changed compared to NitMod2.3 (Garbani, 2014) except for the forward rate constant of all acid-base equilibria which had to be increased from 1000 to 10^8 d^{-1}. This was necessary in order to reach chemical equilibrium in the Matlab implementation within seconds to minutes even after a 1M nitrite pulse addition (see chapter 2.3.3).

2.2. Nitrification reactors

2.2.1. Reactor set-up and operation

For the experiments two 7-liter reactors containing suspended biomass were available (Figure on front page). Stirred at 50 rpm using rectangular stirrer blades (6.9·9.7cm), they were operated as continuous stirred tank reactors (CSTR). They were fed with urine from the BU building of Eawag Dübendorf (the concentration measurements are given in appendix A.2.1).

The inflow was pH-controlled using peristaltic pumps (SCi 400, Watson Marlow). A thermostat (F32, Julabo Labortechnik GmbH) ensured a constant temperature of 25±0.1°C, air control valves (1000 and 4000mln/min, Bronkhorst) a constant air flow into the reactors. The aeration rate, however, was changed several times between 0.09 and 2.2 L/min during the whole operation period; accordingly, the dissolved oxygen concentration was not stable (c.p. appendix A.2). The air was blown into the reactors via ring pipe diffusors.

For the experiments, the aeration was controlled between two oxygen (DO) setpoints using an additional solenoid valve for on/off control. Additionally, the air flowing into reactor used for the experiments was moistened by means of an impinger bottle downstream the air flow controller. In reactor 2, which was used for the experiments, the pH was set to 6.20 / 6.25. During the first two weeks of reactor start-up, the setpoint was gradually increased from 5.9 to 6.35 to enhance the start-up process (c.p. Figure 11 in appendix A.2.

2.2.2. Sampling and analytical methods

During the whole operation period, regular influent and reactor samples were taken. They were taken by means of 25 mL syringes (dissolved samples) and 50 mL syringes (suspended samples).

The dissolved samples were immediately filtered after sampling using micro-glass fibre paper (45µm, MGF, Munktuell Ahlstrom). Once per week, a suspended sample was taken for analysis of total suspended solids (TSS) and volatile suspended solids (VSS) using a 50mL syringe.

The COD, TAN and TNN of the dissolved samples were analyzed photometrically using cuvette test kits (Hach-Lange, Berlin, Germany). Anions (Cl^-, NO_3^-, PO_4^{3-}, SO_4^{2-}) and cations (NH_4^+, $Na^{+,}$, K^+ and occasionally Ca^{2+} and Mg^{2+}) were measured by means of a ion chromatograph (881 Compact IC pro, Metrohm, Herisau, Switzerland). Total inorganic carbon was measured by means of a TIC/TOC analyzer (IL550 OmniTOC, Hach-Lange, Berlin, Germany). The total error of all dissolved measurements including the sample dilutions is assumed to be less than 5%.

The TSS / VSS samples (50ml, 100ml for the calibration experiment) were filtered by using membrane filters for fast filtration (MN640w, diameter 9 cm, Macherey-Nagel). For TSS determination, they were dried in a drying oven at 105°C for at least 1 hour and weighted again after cooling down to ambient temperature. The filters were then glowed in a muffle furnace at 550h for 2 hours to obtain the inert suspended solids (ISS) and VSS as indirect measurement.

Before starting the experiments, TSS and VSS as well as the dissolved reactor concentrations were analyzed. During the experiments, additional samples were taken every 30 minutes using a 7 mL and 15 mL syringe in experiment 1 and 2, respectively. Most samples were analyzed on TNN, some also on TAN, nitrate and other the anions.

The weekly measurements of influent and reactor concentrations of reactor 2 can be found in appendix A.2.2, the measured reactor concentrations prior and during the experiments in appendix A.3.

2.2.3. Continuous measurements

During the whole operation period, pH, dissolved oxygen and the temperature of reactor 2 was measured and recorded every minute on a data logger (Memograph S, RSG40, Endress & Hauser, Reinach, Switzerland). Two pH probes were used: 405-DXK-S8/225 (Mettler Toledo) in reactor 2 and for the calibration experiment; SenTix81 (WTW, Weilheim, Germany) in reactor 1 and for the validation experiment. During the calibration, the measurements were stored every 5 seconds. Optical oxygen sensors (TriOxmatic 700, WTW, Weilheim, Germany) were used. Both DO and pH sensors were regularly calibrated, especially before the experiments. For DO, the calibration procedure by means of water-saturated air was applied. The pH and DO curves in reactor two prior to the calibration experiment are shown in appendix A.2.

2.3. Calibration and validation of NOB growth and decay

2.3.1. Parameter identifiability

Model parameters can only be calibrated if they are identifiable. If, for instance, different linear combinations of parameters lead to the same improvement of the model prediction for a specific experiment, they cannot clearly be identified, and hence not estimated. Accurate estimation of model parameters

therefore necessitates a proper experimental design that allows the distinction of the most sensitive parameters (Gujer, 2008).

2.3.2. Sensitivity analysis of an inflow step

A sensitivity analysis for an inflow step causing a serious nitrite accumulation (120 mg/L within 12 hours) was performed for all growth and decay parameters of AOB and NOB. Starting at steady state with a nitrogen loading rate of 0.13 gTAN/L.d, the loading rate was increased to 1.4 gTAN/L.d. An overview of the simulated reactor concentrations can be found in appendix A.3.

The sensitivity analysis (Figure 1) shows that the most sensitive parameter in this case is the maximal growth rate of NOB (μ^*_{NOB}), followed by the nitrous acid inhibition constant of NOB ($I_{HNO2,NOB}$) and the maximal growth rate of AOB (μ^*_{AOB}). All other parameters turned out to be less sensitive. It was therefore decided to design a first experiment for investigation of the NOB kinetics.
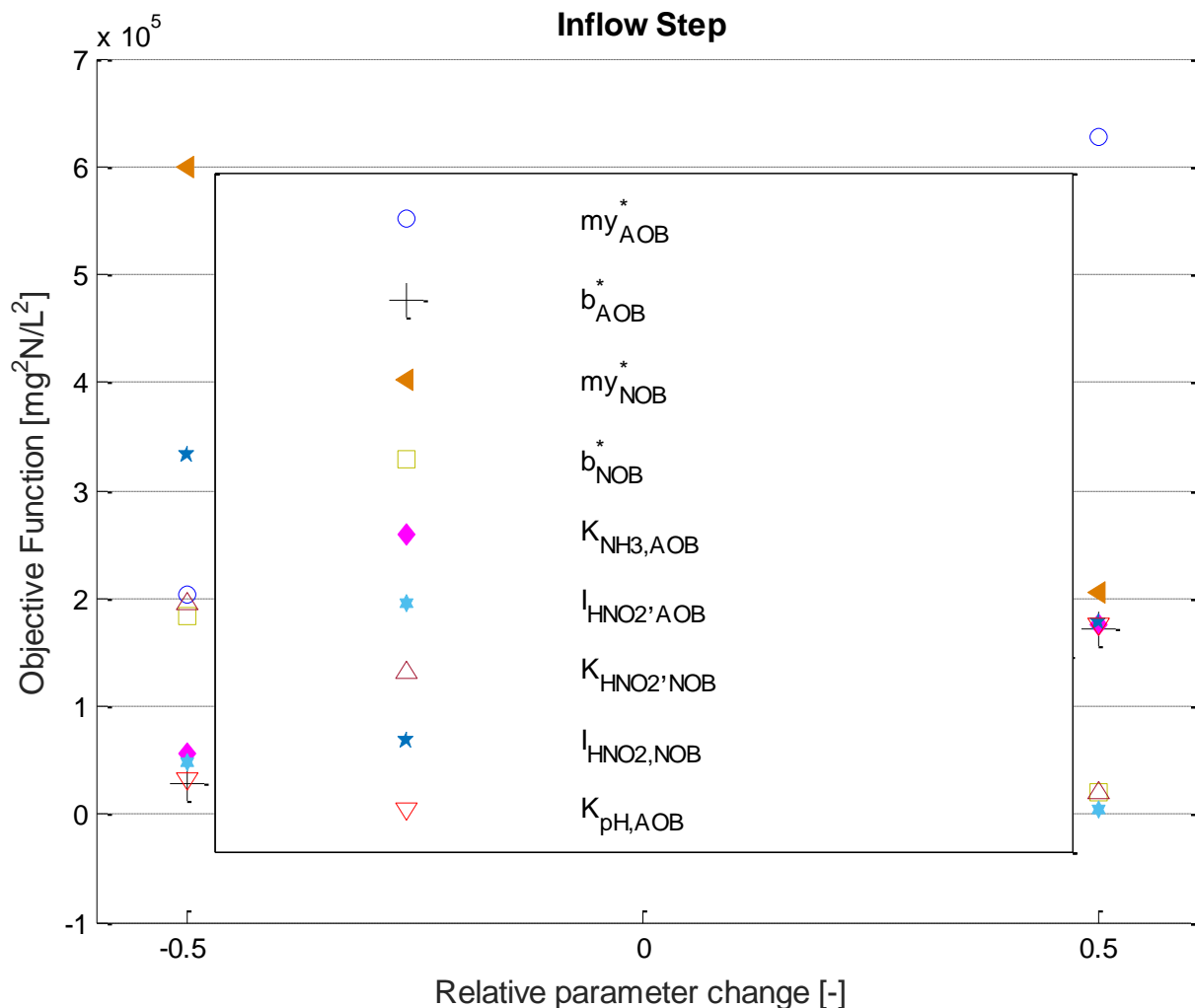

Figure 1: Sensitivity analysis for an inflow step from 0.3 L/d to 3.3 L/d followed by a serious nitrite accumulation. Only the values for a relative parameter change of 50% were calculated.

2.3.3. Calibration experiment

As a calibration experiment suitable to estimate a variety of parameters of NOB, an experimental design of subsequent nitrite pulse additions to endogenous biomass was chosen. Such a design was proposed by (Jubany, et al., 2005) to calibrate the whole parameter set of NOB except for the growth yield by means of respirometric measurement of the oxygen uptake rate (OUR). The identifiability of the whole parameter set was achieved by means of three pulse additions (500 $mgNO_2$-N/L each at pH 7.1±0.02), the second of which was added straight after depletion of the first pulse to assess for biomass growth and the third of which was added 27 hours after complete degradation of pulse 2 to asses for biomass decay.

The calibration experiment for this Master thesis was performed directly in reactor 2 on day 55 after reactor start-up. Up to that point, the reactor had been operated for 1.9 hydraulic retention times at pH 6.25. The nitrogen loading was about 0.25 gTAN/L.d five days before the experiment and 0.15 gTAN/L.d one day before. The influent was turned off 15.7 hours before the first pulse addition. The aeration was controlled between the setpoints 6.0 and 6.2 mgO_2/L during the whole experiment, which allowed the oxygen uptake rate to be measured. Due to a lag of the oxygen sensor, the dissolved oxygen concentration (DO) always exceeded 6.2 mgO_2/L after turning off the aeration; also the slope of the DO decrease between 6.2 and 6.0 mgO_2/L had always reached almost linear values. Due to this fact, the whole range of 6.2 to 6.0 mgO_2/L could be used for respirometric OUR measurement.

The concentrations at the beginning of the experiment are shown in Table 3. For the variables that were expected not to change during the experiment, the average concentration of all measurements (c.p. appendix A.6.1) was used. According to Tchobanoglous (2003), a salinity correction factor of 0.882 had to be applied to all oxygen measurements in order to obtain the true concentration instead of the measured activity.

Table 3: Measured reactor concentrations at start of the experiment. The average concentration is given for the constant variables

Measurement	Method	Concentration [mg/L]
TSS	start	424
VSS	start	404
TAN	average	2240
TNN	start	0.02
NO_3^-N	start	2280
Cl^-	average	2970
PO_4^{3-}-P	average	188
SO_4^{2-}-S	average	706
K^+	average	2070
Na^+	average	1860
Ca^{2+}	1 urine sample	40
Mg^{2+}	1 urine sample	5
TIC	average	<4
Salinity	calculated	21.8

The experiment consisted of four NaNO$_2$ pulse additions (Table 4). Pulse 2 and 3 were added directly after depletion of the previous pulse, between pulse 3 and 4 there was an endogenous period of 13.2 hours, where there was no nitrite in the reactor.

Table 4: Time, volume and concentration of the pulse additions as well as the resulting concentrations in the reactor

	NaNO$_2$ pulse addition			Reactor	
Variable	t	V_{add}	C_{add}	V_R	C_R
Unit	h	mL	mgNaNO$_2$-N/L	L	mgTNN/L
Pulse 1	0.00	20±0.02	14007±14	6.41±0.10	43.5±1.0
Pulse 2	23.85	18±0.04	7004±7	6.15±0.10	20.4±0.5
Pulse 3	28.80	18±0.05	7004±7	6.02±0.10	20.5±0.5
Pulse 4	46.75	20±0.02	5969±6	5.89±0.10	20.2±0.5

The reactors were operated without adding a base that provides alkalinity for (more) complete nitrification (c.p. chapter 2.2.1). Hence, only about half of the TAN was transformed into TNN. This further means that there was a large concentration of untransformed TAN. The alkalinity from the NaNO$_2$ pulses would lead to some AOB activity which is undesired if only NOB kinetics is to be investigated. In order to avoid AOB activity despite the NaNO$_2$ pulse additions, there are basically two options: Either by adding a selective inhibitor for AOB (e.g. allylthiourea, ATU) or by performing the experiment at the low pH limit of AOB.

For the calibration experiment, the second option was chosen. The pH lay at 5.65±0.03 during the whole experiment. There is, however, some pH increase during the first hours after the pulse additions and a general increase between pulse addition 3 and 4 (Figure 2). Figure 2 further shows the decrease of the reactor volume from initially 6.4±0.1 to 5.7±0.1 L at the end of the experiment. The inputs for the uncertainty estimation can be found in appendix A.4.
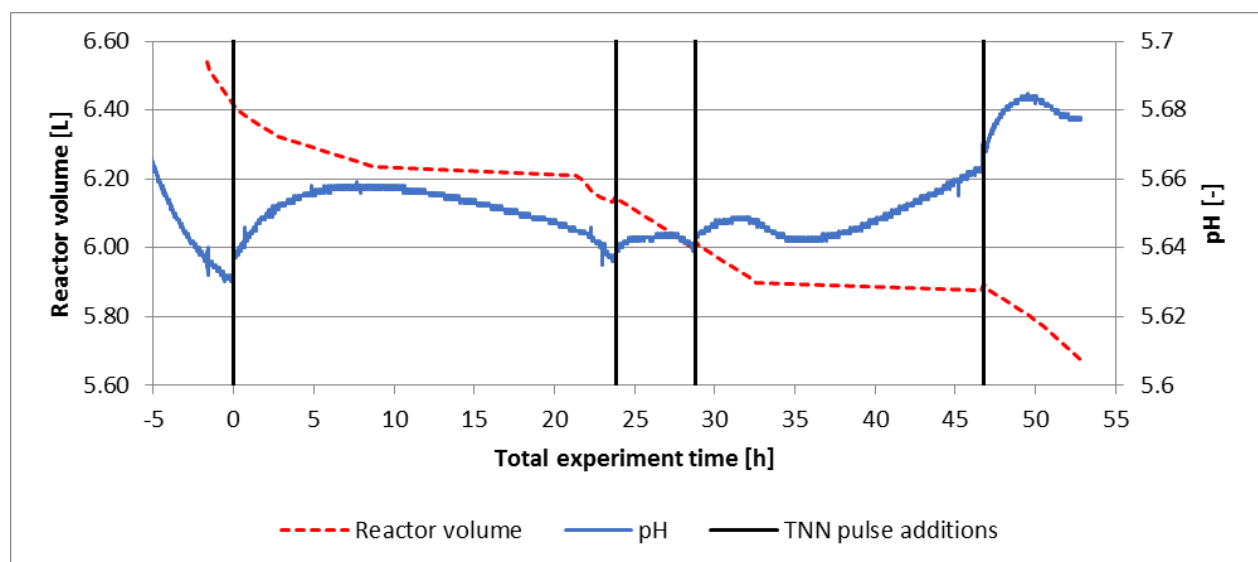

Figure 2: Calibration experiment – reactor volume decreasing due to sampling and measured pH

2.3.4. Calibration experiment: Additional OUR correction

Performing a mass balance for each pulse shows that the measured, non-endogenous oxygen consumption is almost 20% lower than the oxygen needed for complete degradation of all nitrite (inverse of correction factor, c.p. Table 5). However, in order to calculate the nitratation rate from the measured OUR, the TNN mass balance from the non-endogenous oxygen uptake and the added pulse amount needs to be preserved. For this purpose, the measured OUR is multiplied by a factor which is calculated for each pulse individually. The correction factors obtained are listed in Table 5 along with the uncorrected and the corrected endogenous respiration rates. Prior to pulse 1, the same correction factor and endogenous respiration rate as during pulse 1 is used. Subsequent to pulse addition 1, the same OUR correction is always applied up to the next pulse addition and the end of the experiment, respectively. Details about the calculation can be found in Appendix A.5.

Table 5: Measured endogenous respiration rate (OUR$_{end,meas}$) which is used to calculate the correction factor by preserving the nitrogen mass balance. Further listed is the so obtained, corrected endogenous respiration rate (OUR$_{end,corr}$)

	OUR$_{end,meas}$ mgO$_2$/L.d	Correction factor -	OUR$_{end,corr}$ mgO$_2$/L.d
Pulse 1	43	1.20	51.6
Pulse 2	44	1.22	53.9
Pulse 3	46	1.24	57.1
Pulse 4	52.5	1.24	65.3

2.3.5. Modelling the calibration experiment

Since the pH remained at the lower pH limit of AOB (pH 5.65±0.03) during the whole experiment, it was assumed that there was no AOB activity during the whole experiment. The AOB growth term was consequently set zero in the model to avoid nitritation due to pH variations.

As a simplification, all pulses were modelled with a 1M NaNO$_2$ solution. The modelled volumes of pulses 2 to 4 were consequently about 10 mL smaller than the actual pulse additions. By means of using the measured urine volumes at the time of each pulse addition and linearly interpolating them between pulse additions, the resulting volume difference was accounted for.

2.3.6. Using activity peaks for calibration

The activity peaks are of particular interest since they can be used to estimate the initial biomass concentration and additionally either the substrate affinity constant or the substrate inhibition constant.

According to NOB model kinetics (chapter 2.1.1), maximal NOB activity always occurs at the same TNN concentration if environmental conditions stay constant. This is due to the fact that the maximal growth rate (μ^*_{NOB}), the affinity constant ($K_{HNO_2,NOB}$) and the inhibition constant ($I_{HNO_2,NOB}$) as model parameters are independent from the substrate concentration (S_{HNO_2}).

Thus, assuming constant environmental conditions and hence the same substrate concentration at all peaks, the following term reaches the same, constant maximum (k) at every peak:

$$\mu_{NOB}^* \cdot \frac{S_{HNO_2}}{S_{HNO_2} + K_{HNO_2,NOB} + \frac{(S_{HNO_2})^2}{I_{HNO_2,NOB}}} \equiv k$$

Since the vertex of this function is independent from μ_{NOB}^*, one can calibrate either $K_{HNO_2,NOB}$ or $I_{HNO_2,NOB}$ if the substrate concentration at the time of the peaks is known.

The overall process rate of NOB (combined growth and decay, c.p. section 2.1.1) can then be simplified to

$$\rho_{NOB} = (k - b_{NOB}^*) \cdot X_{NOB}$$

Neglecting the oxygen release from biomass degradation at the peak, ρ_{NOB} and the corrected, non-endogenous OUR (OUR$_{TNN}$) become proportional. The ratio of the biomass concentrations of two peaks is therefore given by the ratio of OUR$_{TNN}$ observed at the peak.

$$\frac{X_{NOB,1}}{X_{NOB,2}} = \frac{OUR_{TNN,1}}{OUR_{TNN,2}}$$

If there are at least three subsequent pulses under the same environmental conditions (especially pH and temperature), this equation can be used to find the initial biomass concentration. In the experiment this was assumed to be the case since the temperature was kept constant at 25°C and the pH varied only in a narrow range between pH 5.63 and 5.68. In order to find the optimal biomass concentration from the four activity peaks, the residuals of the model prediction ($OUR_{TNN,model}$) and the OUR given from the sum of squares of the standardized residuals was minimized.

2.3.7. Using OUR measurements for calibration

For model calibration (except for the initial biomass concentration, c.p. section 2.3.6), the OUR measurements reduced by a constant endogenous respiration rate for each pulse were used. As **objective function**, the sum of squared residuals between each measurement and the corresponding model prediction was minimized for either the whole experiment or individual pulses.

2.3.8. Validation experiment

For model validation, a urine pulse experiment was performed on day 48 after reactor start-up, 7 days prior to the calibration experiment using half of the volume of the same reactor. Before the experiment, the reactor had been operated with pH control via the inflow (pH 6.25). It had reached a rather constant inflow rate of 380 mL/d (nitrogen loading rate of 0.22 gTAN/L.d) and then been operated at this inflow rate during 10 days. For the experiment, 3.5 liters of nitrified urine were taken from the reactor for the batch experiment. Prior to adding 50 mL of urine, there was no inflow into the reactor during 36 hours in order to reach the low pH limit of the AOB population (pH 5.75). Due to sampling (7 or 15 mL every hour), the volume decreased from 3.55 L to 3.48 L at the end of the experiment.

The measured concentrations of the urine is given in appendix A.6.2. The average influent concentration measured between 23.2 and 16.3.2015 was used as urine concentration.

2.3.9. Modelling the validation experiment

In order to estimate the initial biomass concentration of AOB and NOB, the model was run with a stable nitrogen loading rate of 0.22 gTAN/L.d until steady state was reached. Afterwards, the period of 36 hours without influent was simulated in order to account for biomass decay. For all simulations a constant volume of 3.5 liters was used to obtain the initial state. The volume decrease was taken into account by linearly decreasing it.

3. Calibration

3.1. Calibration experiment

Figure 3 depicts the course of the measured oxygen uptake rate (OUR) and the TNN concentration during the experiment, both of which are used for model calibration. The TNN measurements suggest that during the first three hours after the first $NaNO_2$ pulse addition, no significant TNN decrease occurs. However, the step increase of the OUR from 53 to about 66 mgO_2/L.d indicates that there is still TNN degradation, despite the strong inhibition occurring at the measured concentration of 43.5 mgTNN/L at the time of the first pulse addition (0.13 mg HNO_2/L at pH 5.66 with $pK_{a,HNO2/NO2^-}$ = 3.25). Subsequent to the pulse additions 2 to 4 with about half the concentration, no such inhibition of the NOB is observed.
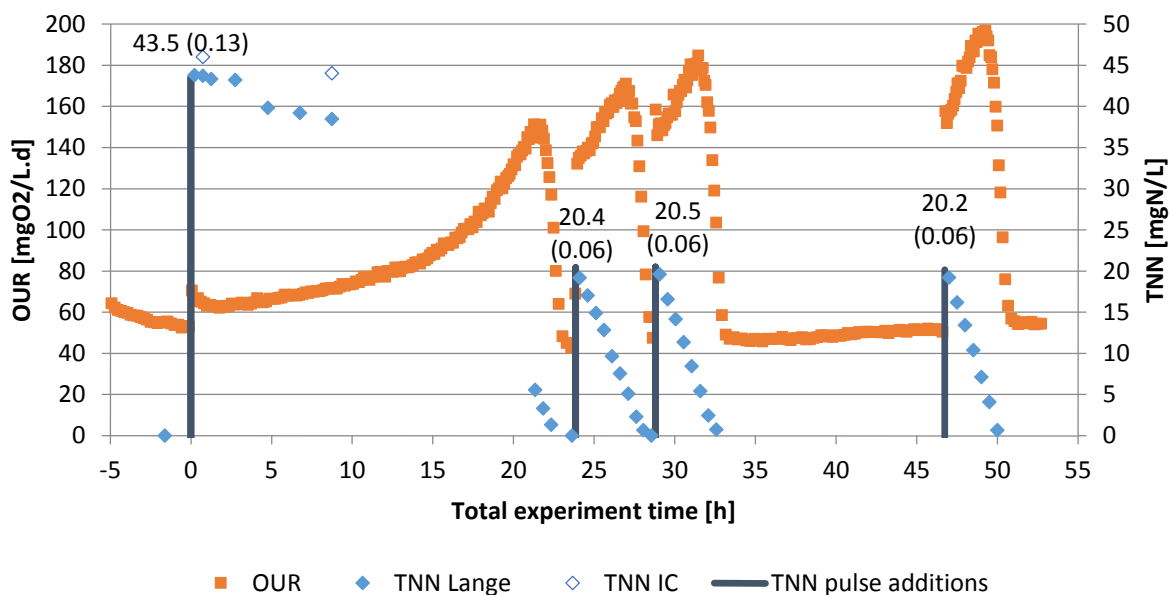
Figure 3: Calibration experiment – measured oxygen uptake rate (OUR) and TNN concentrations in the reactor. Bars: NaNO2-N pulses labelled with corresponding concentration in mgTNN/L and mgHNO₂/L (in brackets)

Remarkable is the drop of the OUR at the beginning of the experiment from 70 mgO_2/L.d (first measurement, 6 min after pulse) to 65 mgO_2/L.d (second measurement, 17 min after pulse), followed by a further decrease until 1.8 hours after the pulse.

The endogenous OUR when no TNN is in the reactor range from 43 mgO_2/L.d before pulse 2 to 54 mgO_2/L.d at the end of the experiment; the minimum before pulse 1 (53 mgO_2/L.d) lies significantly above the OUR measured directly before pulse 2 (43 mgO_2/L.d). In the course of the experiment, the minimal OUR rises again: it lies at very similar levels of 46 and 47 mgO_2/L.d after complete degradation of pulse 2 and pulse 3, respectively, and recovers to 51 mgO_2/L.d during the 13 hours until pulse 4 is added.

The TAN concentration stays at a constant level of about 2200 mgTAN/L during the whole experiment, the nitrate concentration at about 2300 $mgNO_3$-N/L. The nitrate measurements (especially by IC) suggests a slight increase of the nitrate concentration by some 100 $mgNO_3$-N/L, which lies in the same range as the sum of all $NaNO_2$ pulse additions (105 $mgNO_2$-N/L). The results are shown in Figure 14 in appendix A.6.1.

3.1.1. Corrected OUR

Figure 4 displays the course of the corrected OUR (c.p. chapter 2.3.4) together with the measured OUR and the (corrected) endogenous respiration rates for each pulse.
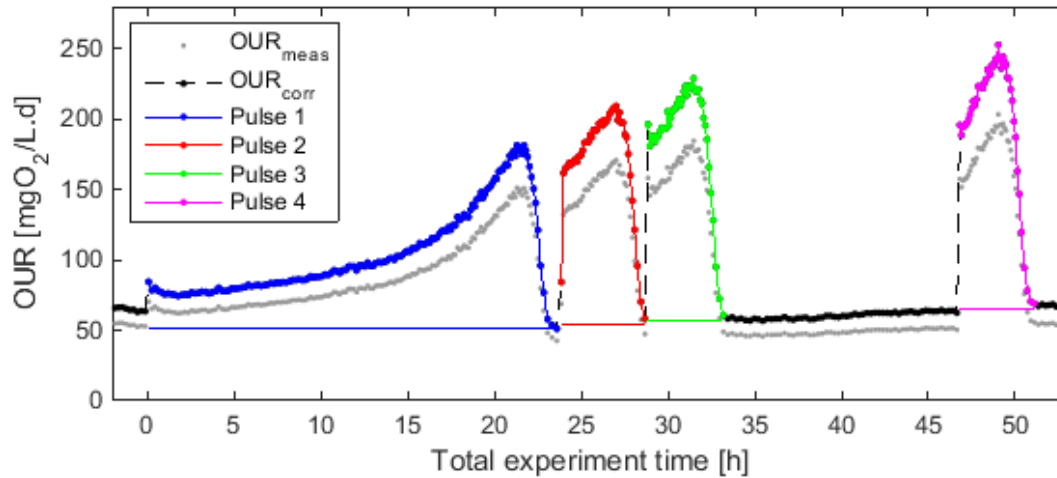
Figure 4: Measured (gray) vs. corrected (black / colored) OUR. The area between the endogenous respiration rates (colored lines) and the corrected curves corresponds exactly to the oxygen demand needed to transform the nitrite pulse additions into nitrate.

3.1.2. Activity peaks

The activity peaks were used to estimate the initial biomass concentration and to obtain an alternative estimate of the inhibition constant. Table 6 gives the TNN concentrations together with the time of peak occurrence as well as the corresponding maximal OUR (corrected). Uncertainty calculations are found in appendix A.4.

Table 6: OUR peaks: Time of peak occurrence, corresponding OUR ($OUR_{max,corr}$) and measured TNN concentration (linear interpolation). The uncertainty range of TNN takes into account the uncertainty of both the TNN measurement itself (±5%) as well as the uncertainty of the time of peak occurrence (±10min)

	Time of peak	$OUR_{max,corr}$	TNN
	h	mgO$_2$/L.d	mgN/L
Pulse 1	21.31±0.13	182	5.8±1.1
Pulse 2	27.02±0.13	209	5.5±1.1
Pulse 3	31.49±0.13	229	5.9±1.1
Pulse 4	49.29±0.13	245	5.4±1.1
Pulse 4 (max.)	49.03±0.13	253	7.0±1.1
Average (without max. of pulse 4)			5.7±0.6

3.2. Step 0: Initial biomass concentration from activity peaks

By optimizing the ratios of the activity peaks (c.p. chapter 2.3.6), an initial biomass concentration of **$X_{NOB}(0)=0.0050$ gCOD/L** with an uncertainty range within **0.0040 and 0.0065 gCOD/L** was estimated. The uncertainty range was calculated by assuming a maximal deviation of the non-endogenous OUR peaks of 4%. Detailed calculations can be found in appendix A.7.1.

The results with the uncertainty range of $X_{NOB}(0)$ are given in Figure 5 for the OUR and Figure 20 for the TNN and the modelled biomass concentration. Figure 5 shows that there is an increasing maximal activity peak with each pulse. Due to the calibration procedure, the ratios of the modelled non-endogenous OUR peaks are the same as the observed ones. However, the model overestimates NOB activity during the first hours of pulse 1 for the whole range of initial biomass concentrations. Furthermore, the model underestimates biomass activity after this time, even with the upper $X_{NOB}(0)$. This goes together with the fact that in the model, pulses 3 and 4 are depleted less rapidly than actually observed and pulse 2 is not degraded at all before pulse 3 is added.
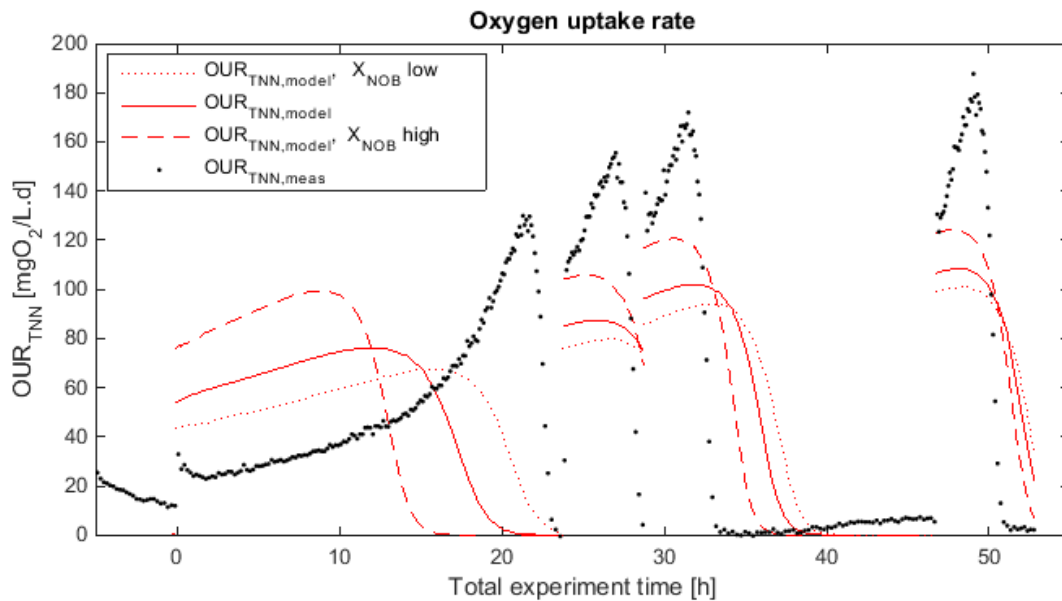
Figure 5: Modelled non-endogenous OUR (OUR$_{TNN}$) for a sensitivity range of $X_{NOB}(0)=0.0040 - 0.0050 - 0.0065$ gCOD/L compared to the measured, non-endogenous OUR

The same pattern can also be seen in the graph with the TNN concentrations (Figure 20 in appendix A.7.4).

3.3. Step 1: Estimation of $K_{I,HNO2,NOB}$

Using the initial biomass concentration, another sensitivity analysis was performed. For the objective function of all pulses, the best improvement results for an inhibition constant $I_{HNO2,NOB}$ lowered by 73%; although, the objective value can only be reduced by 6% to (c.p. Figure 17 in appendix A.7.3).

Much better improvements are achieved when looking at the individual pulses: The sensitivity analysis for pulse 1 reveals that the best improvement (objective function -83%) can be achieved in this pulse by reducing the inhibition constant $I_{HNO2,NOB}$ by 75% (Table 7). A similar improvement is obtained for the following pulses if the maximal growth rate μ^*_{NOB} is increased by 40% (objective value -73%, -87% and -81% for pulses 2, 3 and 4). Changing any other parameter value yields smaller improvements.

Table 7: Parameter changes that result in the best improvement of the objective function: $I_{HNO2,NOB}$ (for pulse 1) and μ^*_{NOB} (for pulses 2-4) for a low, an average and a high initial biomass concentration as found in section 3.2. However, only one parameter can be estimated from the peaks. The values are given for a temperature of T=25°C.

$X_{NOB}(0)$	$I_{HNO2,NOB}$	$\mu^*_{NOB}/\exp\left(\dfrac{-8183}{273+T}\right)$
gCOD/L	mol/L	d^{-1}
0.0040	$1.1\cdot10^{-4}$ (-65%)	$8.5\cdot10^{-5}$ (+60%)
0.0050	$8.0\cdot10^{-5}$ (-75%)	$7.5\cdot10^{-5}$ (+40%)
0.0065	$4.5\cdot10^{-5}$ (-86%)	$6.9\cdot10^{-5}$ (+30%)

The sensitivity analysis for the pulses with the maximal improvement (pulse 1 and 3) are shown in Figure 6, additional plots can be found in appendix A.7.3.
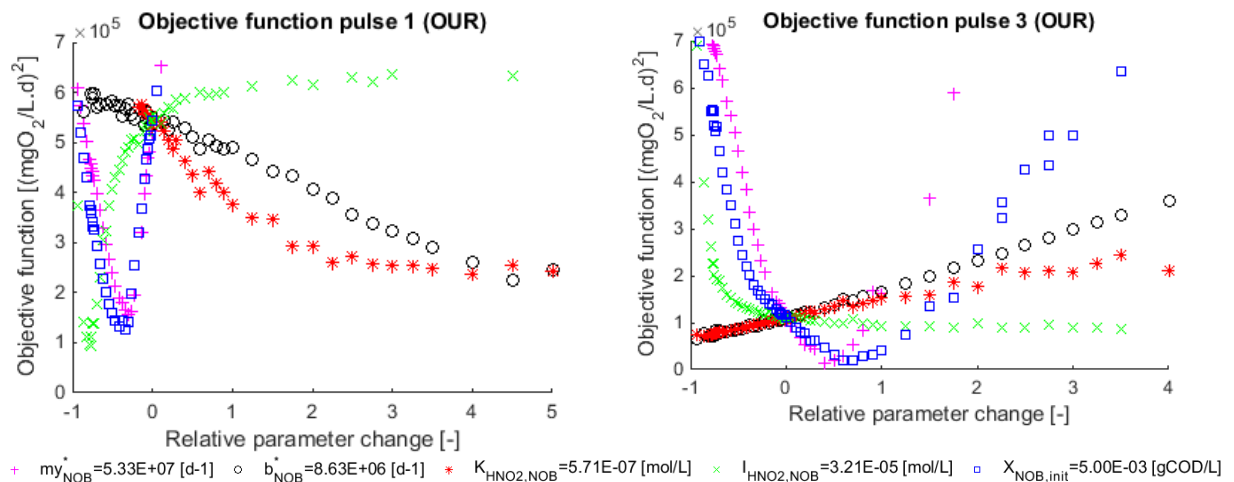
Figure 6: Sensitivity analysis for $X_{NOB}(0)$ = 0.005 gCOD/L for pulse 1 (left) and the pulse 3 (right). The data points for lowered $K_{HNO2,NOB}$ on the left side are missing due to numerical problems in Matlab; the values, however, further increase with decreasing $K_{HNO2,NOB}$ due to larger residuals (c.p. reduction of 75% in Figure 7)

For pulse 1, any parameter reaches a minimum within a range of minus 0.8 to plus 5 parameter change (Figure 6 on the left): The resulting NOB activities for each improvement are shown as non-endogenous OUR in Figure 7.

- Reducing $I_{HNO2,NOB}$ by 75% leads to an optimal improvement (-83%) as stated above.
- A decrease of μ^*_{NOB} by 35% results in a reduction of the same order of magnitude (-77%).
- Increasing the decay constant b^*_{NOB} by 450% has a similar effect as lowering μ^*_{NOB} during the first pulse. Nevertheless, this minimum leads to an overall decrease of the NOB activity during all pulses. This means that the NOB concentration decreases despite of the pulse additions.
- If the substrate affinity constant $K_{HNO2,NOB}$ is increased by 400%, the shape of the OUR curve during pulse 1 worsens: The peak is no longer pointed as it was observed. This pattern is much better achieved with $K_{HNO2,NOB}$ being decreased by 75%, which is also valid for the other pulses. It corresponds to the best qualitative improvement (pointed shape of activity curves) besides the reduction of $I_{HNO2,NOB}$; there is almost no rise in the initial activity when $K_{HNO2,NOB}$ is decreased by 75%. With such a parameter change, the rather quick decline of the biomass activity after the peaks is much better represented.

In both pulses, μ^*_{NOB} and $X_{NOB}(0)$ as well as b^*_{NOB} and $K_{HNO2,NOB}$ have the same pattern in terms of objective function. b^*_{NOB} and $K_{HNO2,NOB}$, however, do not have a clear optimum, for pulse 3 the minimum for both is reached at parameter values of almost zero.
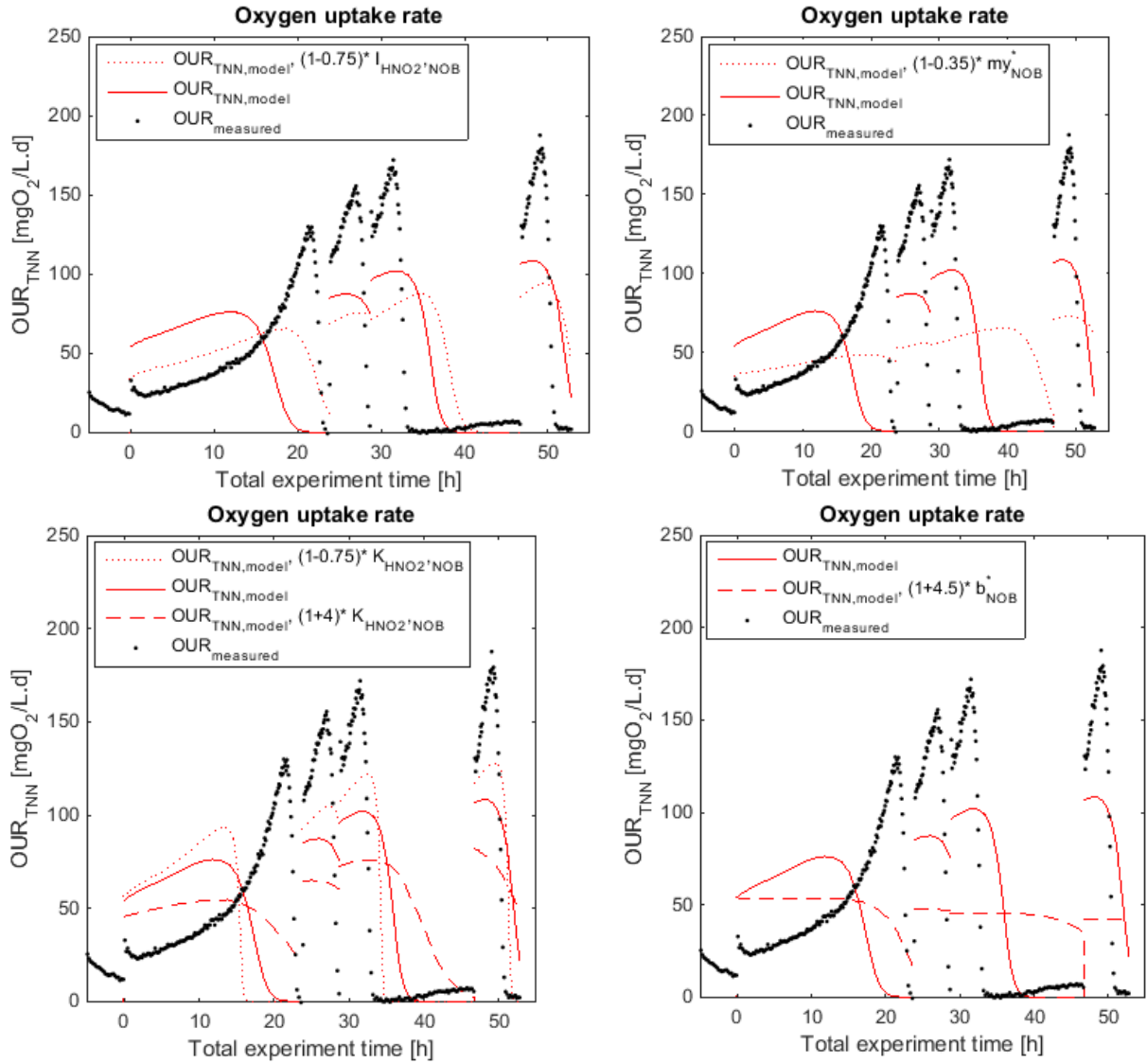
Figure 7: Modelled and measured non-endogenous OUR for the original parameter value and the parameter value that results in the best improvement of the objective function. – Upper left: Reduction of $I_{HNO2,NOB}$ by 75%. – Upper right: Reduction of μ^*_{NOB} by 35% – Lower left: Relative change of $K_{HNO2,NOB}$ by -0.75 and +4 – Lower right: Relative increase of b^*_{NOB} by 4.5.

3.3.1. Alternative estimation of $K_{I,HNO2,NOB}$ or $K_{S,HNO2,NOB}$ from activity peaks

The HNO_2 affinity constant ($K_{HNO2,NOB}$) and the HNO_2 inhibition constant ($I_{HNO2,NOB}$) were also estimated from the TNN concentration at the activity peak (c.p. chapter 2.3.6). However, because of collinearity of both parameters when using this method, only one of them can be estimated; the other one must be assumed given. It was therefore kept at the original value. The so obtained parameters taking into account the uncertainty of the HNO_2 concentration are shown in Table 8. The values correspond to a 91 to 95% increase of $K_{HNO2,NOB}$ and the same decrease for $I_{HNO2,NOB}$, respectively.

Table 8: HNO$_2$ affinity ($K_{HNO2,NOB}$) and inhibition ($I_{HNO2,NOB}$) constants estimated for the minimal, the average and the maximal expected HNO$_2$ concentration

	Unit	Min	Average	Max
S_{TNN} (peak activity)	mgTNN/L	5.0	5.7	6.3
S_{HNO2} (peak activity)	molHNO$_2$/L	9.9E-07	1.2E-06	1.3E-06
$K_{S,HNO2,NOB}$	molHNO$_2$/L	3.0E-08	4.1E-08	5.3E-08
$K_{I,HNO2,NOB}$	molHNO$_2$/L	1.7E-06	2.3E-06	3.0E-06

Figure 8 shows the Haldane term for HNO$_2$ affinity and inhibition for the obtained parameter values (left side) and the reaction rate relative to the maximum on the right side. The sensitivity range is only displayed for the inhibition constant since the deviations for the affinity constant are negligible (<2%) at concentrations above 3 mgTNN/L. They are only relevant (>10%) below 0.4 mgTNN/L whereas for the inhibition constant they exceed a 10% threshold at TNN concentrations larger than about 8 mgTNN/L (c.p. appendix A.7.6).

Figure 8 on the right side further indicates the reaction rates 8.4 and 9.6 minutes after pulse additions 2 and 3, respectively, relative to the reaction rates measured in the preceding peak (2.7 and 1.9 hours earlier for pulse 2 and 3, respectively). The assumption is a constant biomass concentration at the peak and the subsequent pulse addition. The calculations and a simulation using the estimate of $X_{NOB}(0)=0.0050$ can be found in appendix A.7.6.
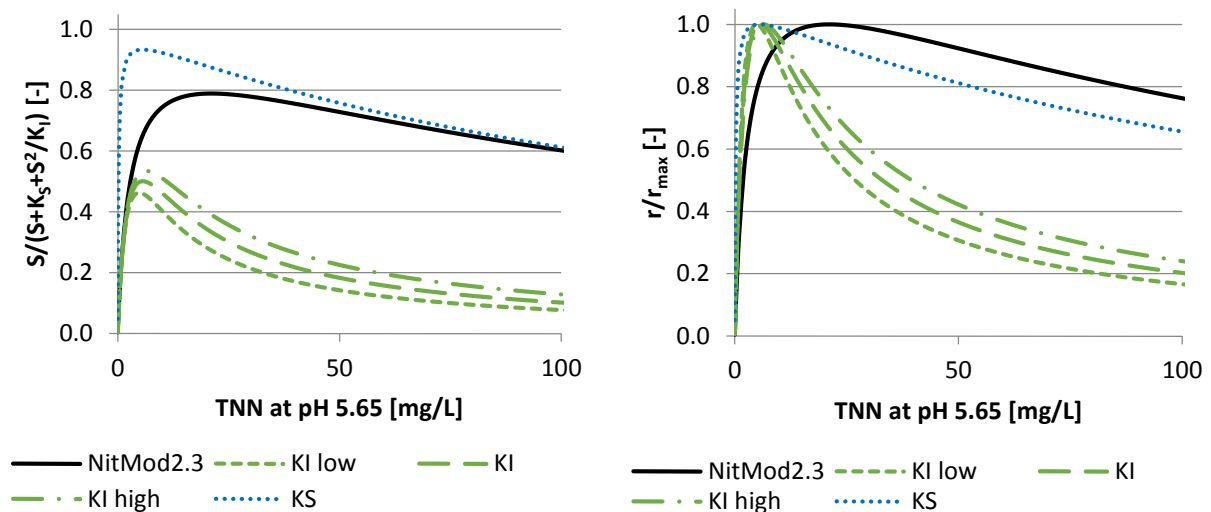
Figure 8: Left: Monod affinity-inhibition (Haldane) term for estimation of $K_{S,HNO2,NOB}$ and $K_{I,HNO2,NOB}$, respectively, using the other parameter from NitMod2.3 for which the term is also shown. – Right: Reaction rate relative to the maximum for NitMod2.3 and the same parameter estimates as on the left.

4. Model validation

The results for the validation experiment are shown in Figure 9. Besides an almost negligible increase of the modelled peak concentration (7.77 to 7.85 mgTNN/L), no improvement can be achieved: In both cases, the pulse is degraded at a faster rate in the beginning. At the end, the modelled decrease seems to be flatter than observed.
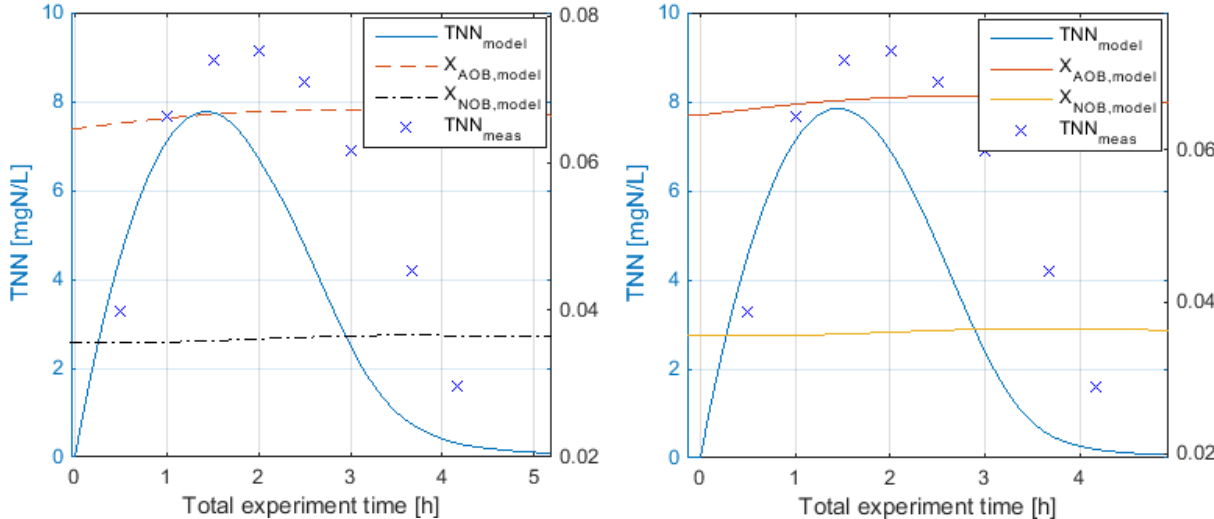
Figure 9: Results for the calibration experiment without (left) and with reduction of $I_{HNO2,NOB}$

5. Discussion

5.1. Measurements during calibration experiment

5.1.1. Oxygen uptake rate

The observation of a decreasing OUR during the first 1.8 hours of the experiment (see section 3.1) and the drop of the endogenous respiration rate during pulse 1 questions the applicability of a constant endogenous OUR in the case of TNN concentrations as added in the experiment. The decrease of the endogenous OUR from 53 $mgO_2/L.d$ (before pulse 1) to 43 $mgO_2/L.d$ (before pulse 2) is a strong indication that endogenous processes are inhibited by excessive TNN concentrations (43.5 mgTNN, corresponding to 0.13 $mgHNO_2/L$). The fact that the endogenous OUR recovers to its initial value during the following 24 hours when the maximal TNN concentration does not exceed 0.055 $mgHNO_2/L$ demonstrates that the inhibiting effect starts to be relevant somewhere between 0.055 and 0.13 $mgHNO_2/L$. It probably also takes some hours until the inhibiting effect fully establishes because the OUR is reducing during the first 1.8 hours.

In addition to the salinity correction, a further OUR correction is necessary in order to preserve the mass balance. This factor of about 1.2 corrects the OUR measurements in the opposite direction of the salinity correction, which is 12%. Reasons for this imbalance may be unsuitability of the applied salinity correction to urine, which not only contains chloride. As the oxygen sensors were calibrated with water-saturated air, there might be a systematic error due to the calibration procedure. Probably, there is also some surface aeration, which lowers the OUR that is measured only some centimeters below the surface.

5.2. Model calibration

5.2.1. Suitability of calibration experiment

The applied experimental design of subsequent nitrite pulses added during endogenous respiration has different advantages to calibrate NOB kinetics:

1) When combined with OUR measurements and a known endogenous OUR, the ratios of the biomass concentrations at the peak are clearly identifiable. Thus the initial biomass concentration can be estimated.
2) If additionally, the substrate concentration at the time of the activity peak is known, one may calibrate either the affinity or the inhibition constant since the activity peak always occurs at the same concentration (c.p. chapter 2.3.6). However, one parameter value must be given. It can for instance be calibrated with all OUR data for an individual pulse or all pulses.
3) If one pulse is added immediately after a depletion of the previous one and another pulse is added several hours after depletion of the previous one, the maximal growth rate and the decay constant can also be distinguished.

Despite these advantages, one must always take into account for the uncertainties. The major uncertainty in the calibration experiment arises from the initial biomass concentration (section 5.2.3), which

has a strong influence on all other parameters that are estimated from the OUR data set. Further uncertainties include the measurements themselves (calibration of the DO and pH sensor as well as analyzed sample) and surface aeration, which depends on the surface area and the mixing conditions.

5.2.2. Objective function and calibration procedure

As obvious from Figure 7 on page 17, not all optima of the objective functions do correspond to an improvement of the modelled behavior of biomass activity. For instance, the lowest objective function value for the affinity constant $K_{HNO2,NOB}$ drastically deteriorates the course of the OUR; however, decreasing the parameter value by 75% brings about a more rapid growth rate in the beginning. As a result, a similar peak pattern evolves as the one observed. Due to the more rapidly increasing growth rate, the nitrite is depleted several hours earlier than in reality. Thus, the sum of the squared deviations becomes much larger than in the case of increasing the parameter value.

This example demonstrates the need to set a realistic parameter range in advance in order to find the most likely parameter set, which is particularly true when automatic minimisation of the objective function is applied. By means of the Fisher Information matrix, such probable parameter ranges could be identified. Alternatively to automatic optimisation, one may estimate parameters iteratively and verify for each estimate whether the minimization of the objective function also leads to convergence of the modelled to the real evolution of the concentrations. This was done in a first calibration iteration for estimation of $I_{HNO2,NOB}$.

In terms of objective function, it would be more practical to use e.g. the root mean square deviation of the single measurements instead of the sum of all measurements. This would facilitate comparing the improvements of different sequences during the experiment and help to reveal the periods with the highest sensitivity for specific parameters.

5.2.3. Estimation of initial biomass concentration (Step 0)

Estimating the initial biomass concentration X(0) is one of the major issues in calibrating biological models because it is completely correlated with the maximal growth rate (μ^*) and further correlated with the decay rate (b^*) under normal operation conditions. Hence, it is not identifiable unless a proper experimental design is applied. The design of the performed calibration experiment with subsequent nitrite pulses is suitable for this purpose if the peak activity is measured, e.g. using OUR measurements with a high temporal resolution (c.p. section 5.2.1). The precision of a single OUR measurement and the accuracy of the endogenous respiration rate are then the only factors affecting the accuracy of the biomass estimate, which is a great advantage of this design.

The simulation with the range of the biomass concentration (Figure 5, page 15) clearly shows that NOB kinetics cannot properly be modelled at the investigated lower pH limit of AOB. The inhibition constant needs to be strongly reduced (about a factor 4) and the maximal growth rate to be increased in order to better model the low biomass activity at large HNO_2 concentrations.

It depends on the pulse concentration and the timing of the pulse additions, to what extent these parameters can be identified. Generally, the estimate of X(0) and μ^* gets better the larger the pulse concentrations are (as long as inhibition remains below a certain threshold) whereas b^* is only identifiable when adding a pulse after an endogenous period of adequate duration.

As mentioned in section 3.3, the initial biomass concentration and the maximal growth rate of NOB are strongly correlated in the experiment.

5.2.4. Estimation of $K_{I,HNO2,NOB}$ from OUR measurements (Step 1)

In terms of the objective function for all pulses, $I_{HNO2,NOB}$ yields the best improvement. However, the objective value only decreases by 6%. Compared to the amelioration achieved by estimating $I_{HNO2,NOB}$ from pulse 1 and μ^*_{NOB} from pulses 2-4, which lie in the range of 80%, this is almost negligible. The estimate of $I_{HNO2,NOB}$ is in fact an overlap of a strong improvement for pulse 1 (due to inhibition) and a moderate deterioration for each of the subsequent pulses. The opposite is true for the μ^*_{NOB} estimated from pulses 2-4. Consequently, μ^*_{NOB} can best be estimated from pulses 2-4, $I_{HNO2,NOB}$ from pulse 1. Comparing the OUR of the objective minima of μ^*_{NOB} and $I_{HNO2,NOB}$ both for pulse 1 indicates that this pulse cannot be used to estimate μ^*_{NOB}; by means of the objective function, only estimating $I_{HNO2,NOB}$ leads to a meaningful improvement.

The first pulse of the calibration experiment reveals that for a decrease of $I_{HNO2,NOB}$ by 75%, the NOB activity at the 0.13 mgHNO$_2$/L is still overestimated compared to the corrected OUR. Adding a constant correction term instead of multiplying the OUR data by a factor would result in an improvement of the fit for the estimated $K_{I,HNO2,NOB}$.

A better fit of large inhibition at high HNO$_2$ concentrations as well as a fast reaction rate at low concentrations may be obtained by lowering the substrate affinity constant. However, it could also be due to poor behavior of the inhibition term at the low pH of 5.65.

From the amelioration of the pulse pattern when lowering $K_{HNO2,NOB}$ follows that in a further calibration step also this parameter may need to be reduced. However, it cannot be concluded from the modelled OUR whether this improvement of the pulse pattern stems from an overestation of $K_{HNO2,NOB}$ or of an overestimation of b^*_{NOB}; linear combinations of both changes will also result in the same improvement. This indicates that $K_{HNO2,NOB}$ and b^*_{NOB} cannot be estimated from the OUR data; they are not clearly identifiable.

5.2.5. Alternative estimation of $K_{I,HNO2,NOB}$ or $K_{S,HNO2,NOB}$ from activity peaks

Nevertheless, an estimate of $K_{S,HNO2,NOB}$ is possible from the TNN concentrations at the activity peaks: If $K_{I,HNO2,NOB}$ is known, $K_{S,HNO2,NOB}$ is identifiable from the activity peaks. This was only done for the original value of $K_{I,HNO2,NOB}$ (and $K_{I,HNO2,NOB}$ from the original $K_{S,HNO2,NOB}$). The resulting reductions of at least 91 to 95% of $K_{I,HNO2,NOB}$ and hence an increase of $K_{S,HNO2,NOB}$ in a similar range are very unlikely. Much more probable is the hypothesis that both parameters should be lower as proposed in section 3.3.

This hypothesis is supported by dividing the first biomass activity measurement after pulse additions 2 and 3 to the maximal activities at the time of the previous and the subsequent peak (maximally 3 hours earlier or later). Figure 10 shows the resulting relative activities, which are larger if divided by the maximal activity of the previous peak (red crosses) and smaller if divided by the maximal activity of the next peak (black crosses). Tables with details about the calculation can be found in appendix 0.
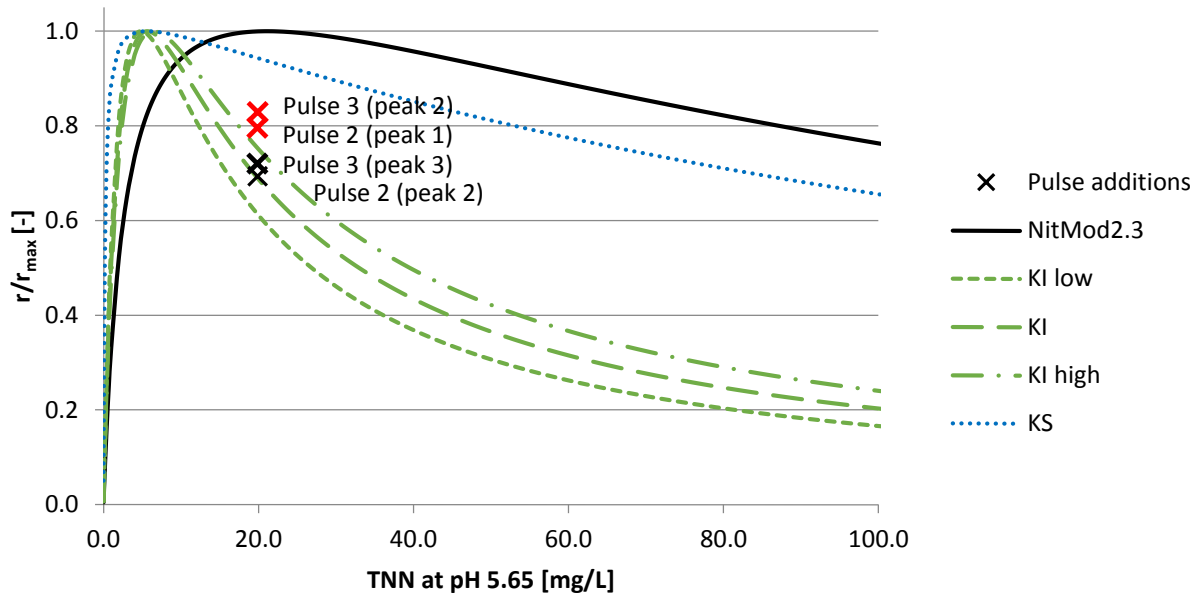
Figure 10: Reaction rate relative to the maximal reaction rate for the Haldane equation of NOB (Figure 8). The NOB activity shortly after pulse addition 2 and 3 relative to the activity at the previous pulse (red crosses) and the subsequent peaks (black crosses). The curve using the initial value is also shown (NitMod2.3).

Since the NOB biomass concentration increased between peak 1, peak 2 and peak 3, it is supposed that the NOB concentration shortly after pulse additions 2 and 3 was larger than at the time of the previous peak, but smaller than at the subsequent peak. Therefore, the curve of the true relative reaction rate passes between the red and the black crosses.

The figure reveals that this is only the case for the upper boundary of the HNO_2 inhibition constant of NOB (KI high, green dash-dotted line, which was estimated from the activity peaks. The uncalibrated parameter set (NitMod2.3, black line) is not able to match between the crosses and further largely overestimates the concentration of the peak activity (21 mgTNN/L instead of 5.7 mgTNN/L). If the HNO_2 substrate affinity constant (KS, blue dotted line) is estimated instead of the inhibition constant KI, the curve approaches the crosses but does not pass between the crosses and is hence not able to reproduce real behavior. Nevertheless, a match is possible if both the inhibition constant and the affinity constant are reduced (not shown). Assuming the Haldane term of NOB correct, the estimate of the inhibition constant (Table 8, page 18) is therefore too low.

5.2.6. Performance in predicting nitrite accumulations

The validation experiment shows that changing only the inhibition constant leads to no improved prediction of the nitrite concentration. There are various possible explanations for this lack of improvement:

- Inaccurate estimation of the initial biomass concentration (of both AOB and NOB): If the modelled decay is lower than in reality, the initial biomass concentration is overestimated due to the 36-hour period without substrate. From the sensitivity analysis it seems that the decay constant should be decreased (as should the affinity constant).
- The maximal measured TNN concentration of about 9 mg TNN/L is too low for the inhibition term to become important. At higher concentrations, the improvement is expected to be larger due to the kinetic term.
- No calibration of AOB kinetics: the maximal growth rate of AOB has a large sensitivity in the initial sensitivity analysis, especially when increased. A larger maximal growth rate of AOB will anyway be needed if the maximal growth rate of NOB is augmented as suggested in chapter 3.3 (looking at pulses 2-4).

6. Conclusions

The calibration experiment shows that the general behavior of NOB in urine nitrification can be modelled by application of the kinetic model and the parameter values proposed by Fumasoli (subm.). However, it reveals that nitrite inhibition is underestimated particularly at HNO_2 concentrations higher than approximately 0.1 $mgHNO_2/L$.

Decreasing the inhibition constant by 75% to $8.0 \cdot 10^{-5}$ $molHNO_2/L$ yields an improved fit at such high concentrations. Meanwhile, the behavior at lower concentrations deteriorates; an increase of the maximal growth rate or a decrease of the substrate affinity constant can explain this to some extent. Another hypothesis for this phenomenon is that the kinetic term does not represent real behavior.

In addition to a decrease of the inhibition constant, the affinity constant needs to be decreased, which is supported by the OUR data as well as the estimates from the TNN concentrations at the time of the activity peaks. Also the maximal growth rate should increase according to the experimental data. No clear statement can be made about the decay coefficient; in the experiment, similar improvements are achieved by either changing the affinity constant or the decay coefficient. Besides this, the poor fit of the experimental data suggests that the inhibition term of the model might not be correct.

Modelling the nitrite pulses experiment revealed that the rate constant of the chemical equilibria need to be chosen large enough in order to avoid erroneous AOB and NOB activities. Otherwise, TAN and TNN may reach chemical equilibrium only after a large delay, e.g. after an increase of the inflow.

7. Outlook

The incomplete fit of the nitrite pulses experiment and the sensitivity analysis of the last step indicate that the NOB kinetics can still be improved by using the same experimental data. It would be worth looking at another inhibition term, e.g. of second order, so that the observed inhibition at high HNO_2 concentrations can be modelled more accurately.

In order to obtain accurate estimates of the maximal growth rate and the decay rate, larger pulse concentrations are needed. This is only possible at higher pH values due to the equilibrium of HNO_2 and NO_2^-. For this purpose, the AOB have to be inhibited by a selective inhibitor (e.g. ATU) or the reactor must be operated at complete nitrification, where the TAN concentration can easily be reduced to zero.

Since the HNO_2 concentration does not reach a critical level during the validation experiment, the model with the improved parameter set should be validated on experimental data where strong inhibition of NOB by HNO_2 occurs.

It would further be interesting to investigate the impact of other factors like the salt concentration, the urine composition and longer operation periods at temperatures above 25°C on the AOB and NOB kinetics.

8. Literature

Etter, B., Udert, K. M. and Gounden, T. 2015. *VUNA Final Report.* Dübendorf, Switzerland : Eawag, 2015.

Etter, Bastian, Hug, Alexandra and Udert, Kai M. 2013. Total Nutrient Recovery from Urine - Operation of a Pilot-Scale Nitrification Reactor. Vancouver, Canada : WEF/IWA Conference on Nutrient Removal and Recovery, 2013.

Fumasoli, A., Morgenroth, E. and Udert, K. M. subm.. Modeling the low pH limit of Nitrosomonas eutropha in high-strength nitrogen wastewaters. *Submitted to Water Research.* subm.

Garbani, Lorenzo. 2014. Urine nitrification system model documentation. Dübendorf, Switzerland : Eawag, 11 2014.

Gujer, Willi. 2008. *Systems Analysis for Water Technology.* Berlin-Heidelberg : Springer-Verlag, 2008. ISBN 978-3-540-77277-4.

Gujer, Willi, et al. 1999. Activated sludge model no. 3. *Water Science and Technology.* 1999, 1999, Vol. 39, 1, pp. 183-193.

Hellinga, C., Van Loosdrecht, M. C.M. and Heijnen, J. J. 1999. Model Based Design of a Novel Process for Nitrogen Removal from Concentrated Flows . *Mathematical and Computer Modelling of Dynamical Systems.* 12 1999, Vol. 5, 4, pp. 351-371.

Jubany, Irene. 2007. Operation, modelling and automatic control of complete and partial nitrification of highly concentrated ammonium wastewater. *PhD thesis.* Barcelona, Spain : Universitat Autonoma de Barcelona, 2007.

Jubany, Irene, et al. 2005. Respirometric calibration and validation of a biological nitrite oxidation model including biomass growth and substrate inhibition. *Water Research.* 11 2005, Vol. 39, 18, pp. 4574-4584.

Jubany, Irene, et al. 2009. Total and stable washout of nitrite oxidizing bacteria from a nitrifying continuous activated sludge system using automatic control based on Oxygen Uptake Rate measurements. *Water research.* 6 2009, Vol. 43, 11, pp. 2761-2772.

Tchobanoglous, G., Burton, F. L. and Stensel, H. D. 2003. *Metcalf & Eddy, Wastewater Engineering - Treatment and Reuse.* Boston : McGraw-Hill, 2003.

Udert, K. M. and Wächter, M. 2012. Complete nutrient recovery from source-separated urine by nitrification and distillation. *Water Research.* 2 2012, Vol. 46, 2, pp. 453-464.

Udert, K. M., et al. 2003. Nitrification and autotrophic denitrification of source-separated urine. *Water Science and Technology.* 2003, Vol. 48, 1, pp. 119-130.

Uhlmann, Corine. 2014. Dynamics of complete and partial nitrification of source-separated urine. *Master Thesis.* Dübendorf : Eawag, 2014.

Van Hulle, S. W.H., et al. 2007. Influence of temperature and pH on the kinetics of the Sharon nitritation process. *Chemical Technology and Biotechnology.* 2007, Bd. 82, S. 471-480.

A Appendix

A.1. Additional model parameters

This section gives all parameter values related to acid-base equilibria, gas exchange and complex formation as applied in the Matlab computer model. The acid-base forward equilibrium rate allKEqConstants = 10^8 had to be increased from 1000 to 10^8 [d-1] in order to reach the chemical equilibrium after a 43 mgNO$_2$-N pulse addition (calibration experiment) within approximately 1-2 minutes instead of several hours.

```
%% Acid-base
parameters.chem.pK_CO3   = 10.33; %[-]
parameters.chem.pK_HCO3  = 6.35; %[-]
parameters.chem.pK_NH3   = 9.24;% [-]
parameters.chem.pK_NO2   = 3.25; %[-]
parameters.chem.pK_H2PO4 = 2.15; %[-]
parameters.chem.pK_HPO4  = 7.2; %[-]
parameters.chem.pK_PO4   = 12.38; %[-]
parameters.chem.pK_SO4   = 1.99; %[-]
parameters.chem.pK_OH    = 14; %[-]

% Forward rates with small k, Equilibrium rate with capital K
allKEqConstants = 10^8;
parameters.chem.k_eq_CO3 = allKEqConstants;  %[d-1]
parameters.chem.k_eq_HCO3 = allKEqConstants; %[d-1]

%% bicarbonate/carbonate-equilibirum
parameters.chem.k_eq_NH3   = allKEqConstants; %[d-1]
parameters.chem.k_eq_NO2   = allKEqConstants; %[d-1]
parameters.chem.k_eq_H2PO4 = allKEqConstants; %[d-1]
parameters.chem.k_eq_HPO4  = allKEqConstants; %[d-1]
parameters.chem.k_eq_PO4   = allKEqConstants; %[d-1]
parameters.chem.k_eq_SO4   = allKEqConstants; %[d-1]
parameters.chem.k_eq_OH    = allKEqConstants; %[d-1]

%% Gas Exchange
parameters.gas.Q_gas   = 1440; %[L·d-1], not necessary
parameters.gas.H_CO2   = 1.2; %[g C(g)/ g C(aq)]
parameters.gas.H_NH3   = 0.00072; %[g NH3-N(g)/ g NH3-N(aq)]
parameters.gas.H_HNO2  = 0.000834; %[g HNO2-N(g)/ g HNO2-N(aq)]
parameters.gas.H_O2    = 32.4; %[g O2(g)/g O2 (aq)], not necessary

parameters.gas.KLa_CO2  = 36.8; %10.0139; % Corresponds to 380 at q=1440 l/d
From fun_Input: 36.7933
parameters.gas.KLa_O2   = 38.73 %10*38.73; %2.6352;  % Corresponds to 100 at
q=1440 l/d From fun_Input: 38.7298
parameters.gas.KLa_NH3 = 1000000;      %large, not effect
parameters.gas.KLa_HNO2 = 1000000;     %large, not effect

parameters.gas.p_CO2    = 0.00039; %0.000335; %[atm] %in C_input is
0.00037793 / Changed by Gabriel (http://www.aqion.de/site/99, 2.3.2015)
parameters.gas.S_O2_sat = 7.9/1000/32; %0.0002578125; %[mol/L]    7.9 mgO2/L
at salinity 0.25% (reactor 2 on 16.02.2015), 440m above sea level at 962.34
hPa air pressure (see Sonden-Log)

parameters.gas.c1       = 0.082057;
parameters.gas.absoluteZeroCelsius = 273.15;
```

```
%parameters.gas.S_CO2_air = parameters.gas.p_CO2/parameters.gas.c1/(parame-
ters.gas.c2+Temperature); %[molC(g)/L] c

parameters.gas.S_NH3_air  = 0; %[molN(g)/L]
parameters.gas.S_HNO2_air = 0; %[molN(g)/L]
parameters.gas.S_O2_water = 8.25/(32*1000); %[mol/L] 8mg O2 equivalent
parameters.gas.S_O2_air   = parameters.gas.S_O2_water*parameters.gas.H_O2;


%% Komplexes
parameters.chem.pK_K2HPO4   = 6.07;    %[-]
parameters.chem.pK_KH2PO4   = -0.3;    %[-]
parameters.chem.pK_KHPO4    = 6.3;     %[-]
parameters.chem.pK_KSO4     = -0.85;   %[-]
parameters.chem.pK_Na2HPO4  = 6.25;    %[-]
parameters.chem.pK_NaH2PO4  = -0.3;    %[-]
parameters.chem.pK_NaHPO4   = 6.13;    %[-]
parameters.chem.pK_NaSO4    = -0.74;   %[-]
parameters.chem.pK_NH4H2PO4 = -0.1;    %[-]
parameters.chem.pK_NH4HPO4  = -1.3;    %[-]
parameters.chem.pK_NH4SO4   = -1.03;   %[-]
parameters.chem.pK_NaCO3    =  -1.27;  % from C_Input, not necessary
parameters.chem.pK_NaHCO3   =  0.25;   % from C_Input, not necessary


parameters.chem.k_eq_K2HPO4   = allKEqConstants; %[d-1]
parameters.chem.k_eq_KH2PO4   = allKEqConstants; %[d-1]
parameters.chem.k_eq_KHPO4    = allKEqConstants; %[d-1]
parameters.chem.k_eq_KSO4     = allKEqConstants; %[d-1]
parameters.chem.k_eq_Na2HPO4  = allKEqConstants; %[d-1]
parameters.chem.k_eq_NaH2PO4  = allKEqConstants; %[d-1]
parameters.chem.k_eq_NaHPO4   = allKEqConstants; %[d-1]
parameters.chem.k_eq_NaSO4    = allKEqConstants; %[d-1]
parameters.chem.k_eq_NH4H2PO4 = allKEqConstants; %[d-1]
parameters.chem.k_eq_NH4HPO4  = allKEqConstants; %[d-1]
parameters.chem.k_eq_NH4SO4   = allKEqConstants; %[d-1]
```

A.2. Reactor operation
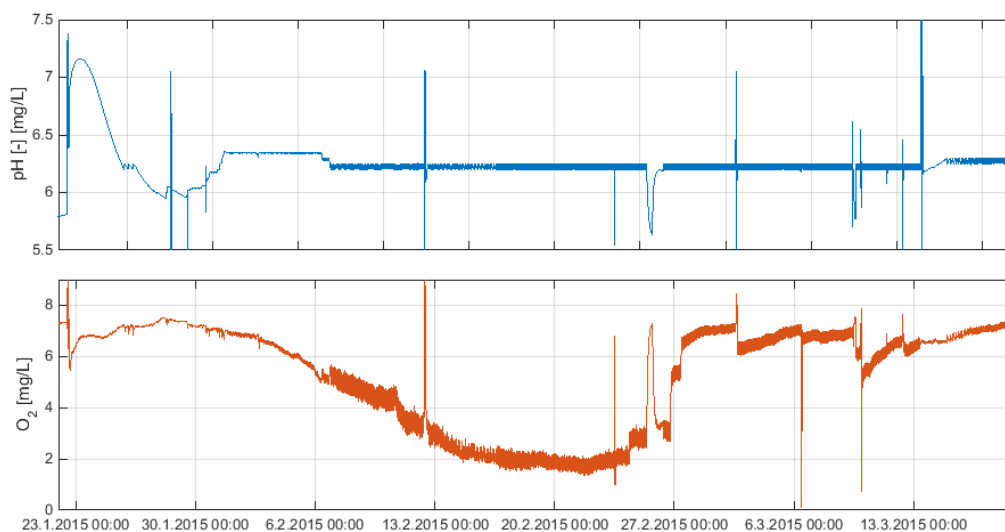
Figure 11: Measured pH and oxygen concentrations in reactor 2 between start up and experiment 2
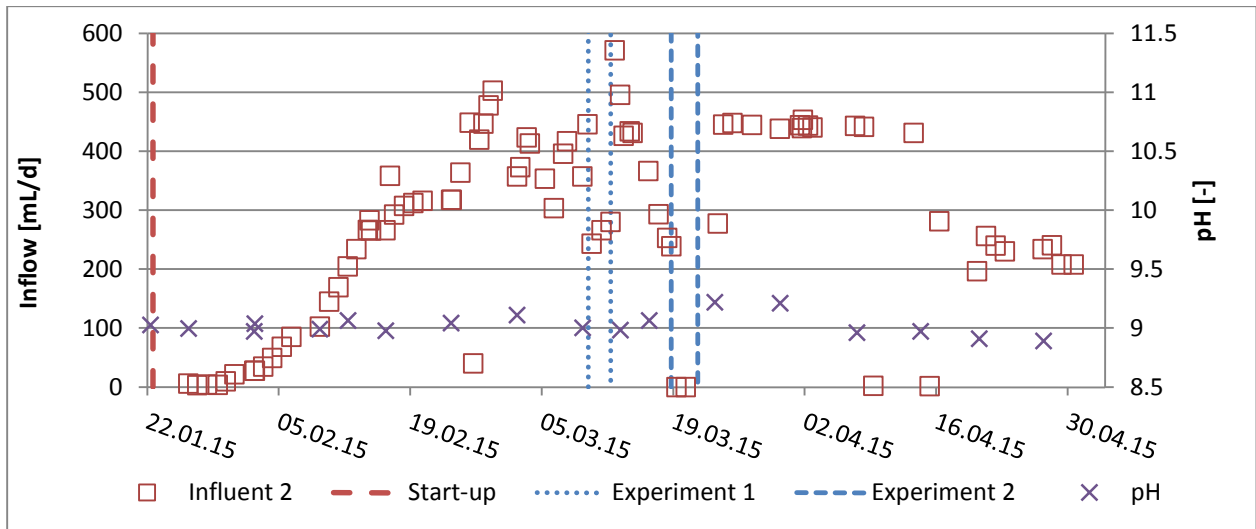
Figure 12: Inflow to reactor 2 which was used for the experiments

A.2.1. Measured influent concentrations

Table 9 shows the measured inflow concentrations to reactor 2 during the operation period.

Table 9: Measured inflow concentrations to reactor 2

Lab.Nr.	Day after start-up	Date	TIC	Cl⁻	PO₄³⁻	SO₄²⁻	TAN	TAN	TAN	COD	Na⁺	K⁺	pH	Re-marks
				IC	IC	IC	Lange	IC	Average	fil.	IC	IC		
			mgC/l	mg·L⁻¹	mgP·L⁻¹	mgSO4·L⁻¹	mgN·L⁻¹	mgN·L⁻¹	mgN·L⁻¹	mgO2·L⁻¹	mg·L⁻¹	mg·L⁻¹		
NF15014	216	05.01 13:30	1787				4100		4100	4300				
NF15027	222	12.01 10:50	1883				4680		4680	4263			9.01	
NF15036	229	19.01 09:35	1830				3940		3940	4431			8.93	
NF15061	236	26.01 10:00	1711	2885	160	580	3620		3620	3200	3200	3100	9.08	
UL15010	250	09.02 09:10	1867	2940	170	630	3900	3965	3933	3480	1690	1590	9.05	
UL15016	257	16.02 09:30	1967	2741	165	534	3900	3970	3935	3450	1689	1481	8.97	
UL15020	264	23.02 09:00	1946	2830	165	555	4110	4160	4135	3175	1775	1540	9.09	old urine
UL15021	264	23.02 09:50	1930	2725	170	550	4140	4200	4170	3450	1800	1530	9.11	new urine
UL15027	271	02.03 09:00	2015	3567	226	3600		4073	4073		1710	1580	9.03	
UL15032	-3	09.03 08:50	2040	2822	182	614	4200	4039	4120	3275	1689	1535	8.98	new buffer soluti-ons: - 0.04 lo-wer
UL15037	1	13.03 09:15	2000	2490	152	496	4080		4080	3175			8.97	
UL15041	4	16.03 11:10	1960	2840	180	610	4280	4120	4200	3100	1720	1520	9.04	
UL15057	11	23.03 10:55	1941	2690	176	550	4100	3490	3795	3725	1435	1360	9.22	
UL15060	18	30.03 09:15	1930	2630			4200	4470	4335	3500	1740	1685	9.26	
UL15063	21	02.04 09:15		2630	180	570	4220		4220	3453			9.23	

A.2.2. Measured reactor concentrations

Table 10 on the next page shows the measured concentrations in reactor 2.

Table 10: Measured concentrations in reactor 2 during the operation period.

Lab. No.	Day after start-up	TIC	Cl⁻	NO₂⁻	Nitrite	NO₃⁻	NO₃⁻	NO₃⁻	PO₄³⁻	SO₄²⁻	NH₄⁺	NH₄⁺	NH₄⁺	COD	COD	Na⁺	K⁺	Ca²⁺	Mg²⁺	pH	Remarks
		IC mgC/l	IC mgN·L⁻¹	IC mgN·L⁻¹	Lange mgN·L⁻¹	IC mgP·L⁻¹	Lange mgP·L⁻¹	Average mgN·L⁻¹	IC mgP·L⁻¹	IC mgS·L⁻¹	Lange mgN·L⁻¹	IC mgN·L⁻¹	Average mgN·L⁻¹	fil. mg·L⁻¹	tot mg·L⁻¹	IC mg·L⁻¹	IC mg·L⁻¹	IC	IC		mg/L
NF15016	216	4.9	3980			2590		2590			2830		2830	391						6.225	
NF15029	222	<4	3750		4.34	2835		2835			3323.3		3323.3	407.4						6.225	
NF15038	229	4.7	3590		229	2530		2530	230	890	2720		2720	708		2170	1770	33	<4	6.225	
NF15047	232		3560			2510		2510	220	890	2630		2630	640		2180	2765			5.8	
NF15064	1	<4	3410		2.31	2330		2330	215	850	2380		2380	392		1910	1560				Matrix from FC men's reactor (6L of new composition)
NF15065	1		2890		3.07	1980		1980	180	700	2040		2040	390						6.9	New bulk composition (incl. 1L activated sludge, SRT = 10d)
NF15063	4	<4	3070		24.1	2240		2240	180	720	2040		2040	376		1665	1240			6.225	
UL15002	7		2870			2130		2130	175	680	2040		2040	284						5.95	
UL15004	8		2880		0.205	2140	2290	2215	175	680	2180		2180	274	643					6.035	
UL15008	11		2920		0.9	2240		2240	165	665	2130		2130	302						6.345	
	14				2.81		2250	2250			2040		2040	294						6.345	
UL15012	18		3140		2.3	2250		2250	200	770	2180		2180	312						6.225	
UL15014	21		2856		4.4	2218		2218	188	660	2240		2240	450						6.225	
UL15018	25		2913		8.2	2233		2233	186	666	2160	2297	2228.5	637.5		1880	1489			6.225	
UL15019	28		3030		4.975	2235	2310	2272.5	200	720	2190		2190	362.5						6.225	
UL15023	32		3020		2.15	2223		2223	190	700	2130		2130	302.5						6.225	
UL15025	35		3770		1.45	2738	2280	2509	238	891	2170		2170	302.5						6.225	
UL15029	39		3923		1.55	2827	2300	2563.5	242	923	2220		2220	312.5						6.225	
UL15030	43		3081		1.675	2270		2270	194	709	2180		2180	302.5						6.225	
UL15033	46	<4	3047		1.525	2244	2490	2244			2230		2230	327.5						6.225	
UL15039	50				1.65			2490			2350		2350							6.225	
UL15043	53	<4	3390			2450		2450	200	790		2200	2200			1870	1680			6.425	
UL15044	56		3000			2180		2180	182	695										6.25	18:45: Influent turned off for calibration experiment
UL15046	56	<4	3020		0.017	2210	2280	2245	185	695	2110		2110	262.5						5.635	
UL15047	56		2940	46	43	2150		2150	180	675										5.64	
UL15048	57		3200	44	38.45	2350		2350	197	735										5.66	
UL15049	57		3050	<20	0.0016	2270		2270	186	710		2295	2295			2030	1870			6.425	
UL15050	58		3050	<20	5.4	2280		2280	187	700										5.635	
UL15051	58		3020	<20	<0.6	2275		2275	187	700										5.64	
UL15052	58		3050	<20	11.35	2300		2300	187	700										5.66	
UL15053	58		3150	<20	2.46	2365		2365	191	715		2250	2250			2060	1840			5.635	
UL15054	58		3170	<20	10.38	2365		2365	190	715										5.64	
UL15055	59		3120	<20	1.54	2380		2380	192	715		2290	2290			2130	1875			5.64	
UL15062	67	6.9	2730		4.3	2105		2105	170	930	2190		2190	331						5.68	
UL15065	70		3050		1.34	2130	2300	2215	195	780	2150		2150	322						6.425	

A.3. Sensitivity analysis
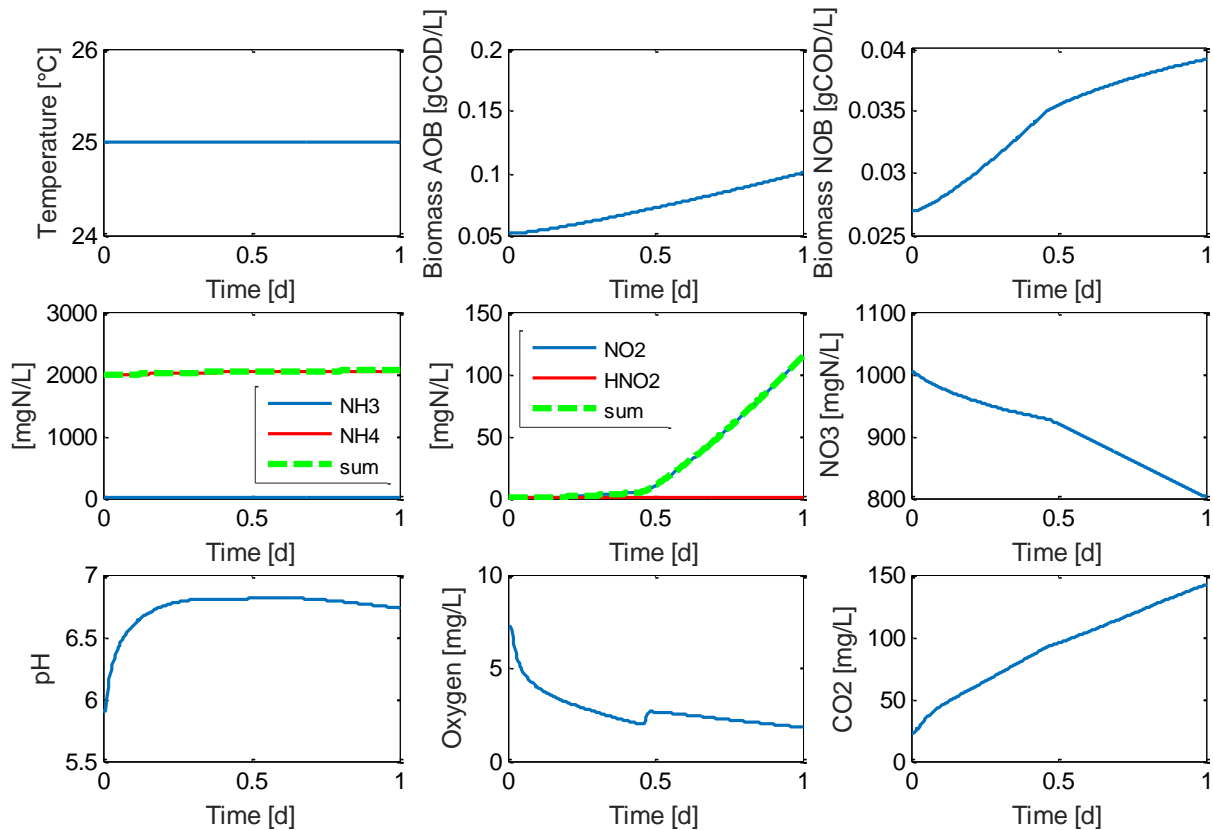
Figure 13: Simulated reactor concentrations in the sensitivity analysis – the nitrogen loading is in steady state (0.13 gTAN/L.d) before time 0, then it is increased to 1.4 gTAN/L.d. After about time 0.5d, NOB start to be strongly inhibited, which results in a slower growth of NOB and a concentration of 120 mgTNN/L about 12 hours later.

A.4. Uncertainty of pulse additions

Table 11: Salt solutions with uncertainty

NaNO₂ Solution No.	Tare weight	Weight with salt	Salt addition	- (>99%)	+	Volume	+/-	Concentration of solution	average uncertainty (volume only)
	g	g	gNaNO₂	gNaNO₂	gNaNO₂	mL	mL	mgNO₂-N/L	mgNO₂-N/L
1	0.9355	4.3854	3.4499	0.034	0.001	50	0.05	14007	14.00
2	0.9029	2.6279	1.725	0.017	0.001	50	0.05	7004	7.00
3	0.9955	2.4657	1.4702	0.015	0.001	50	0.05	5969	5.97

Table 12: Uncertainty of NaNO2-N concentration after pulse addition

	NaNO2 Solution No.	Volume	+/-	V_meas (water head)	V_est = Vinit -Vsampl +Vadd	+/-	Concentration value (V_est)	Uncertainty (V_est) +/-	Uncertainty (total) +/-
		mL	L	L	L	L	mgNO₂-N/L	mgNO₂-N/L	mgNO₂-N/L
Pulse 1	1	20	0.02	6.45	6.414	0.10	43.54	0.73	0.99
Pulse 2	2	18	0.035	6.14	6.152	0.10	20.43	0.38	0.50
Pulse 3	2	18	0.05	5.94	6.019	0.10	20.53	0.40	0.53
Pulse 4	3	20	0.02	5.89	5.894	0.10	20.18	0.37	0.51

A.5. OUR correction

The data used for the OUR correction are given in Table 13.

Table 13: Calculation of the OUR correction factor by minimizing the sum of least squares between real pulse addition P(i) and pulse amount calculated from the measured oxygen uptake (P$_{OU,meas}$) using a constant endogenous respiration rate (OUR$_{end,meas}$) during each pulse. The Correction factor and the corrected endogenous respiration rates are given in the last two colums. Additionally, the number of used data points is indicated.

Pulse addition		Measurements				Correction	
i	P(i)	OU-R$_{end,meas}$	P$_{OU,meas}$	(P$_{OU,meas}$-P(i))^2	No. of data points	Correction factor	OU-R$_{end,corr}$
-	mgTNN/L	mgO$_2$/L.d	mgTNN/L	(mgTNN/L)^2	-	-	mgO$_2$/L.d
1	43.5	43	36.3	53.0	153	1.20	51.6
2	20.4	44	16.7	14.1	44	1.22	53.9
3	20.5	46	16.6	15.8	42	1.24	57.1
4	20.2	52.5	16.2	16.2	43	1.24	65.3

A.6. Experimental results

A.6.1. Calibration experiment

Figure 14 shows the development of TAN and nitrate during the calibration experiment.
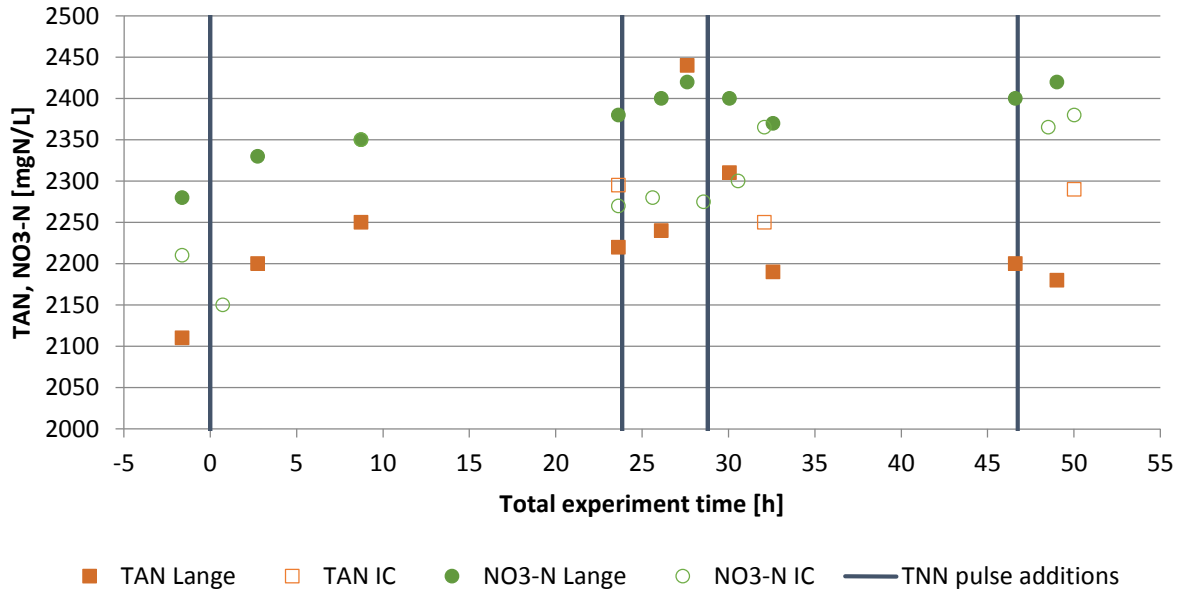

Figure 14: Calibration experiment – measured TAN and NO3-N concentration

Table 14 contains all the measurements. All nitrite analyses by Dr. Lange with their analysis times (storage in fridge) are given in Table 15 on the next page.

Table 14: Analyzed reactor concentrations during the calibration experiment

Time	Biomass TSS	VSS	IC measurements TAN	NO2	NO3	Cl-	PO4	SO4	K+	Na+	Lange measurements TAN	TNN	NO3	CODdiss
h	mg/L	mg/L	mgN/L	mgN/L	mgN/L	mg/L	mgP/L	mgS/L	mg/L	mg/L	mgN/L	mgN/L	mgN/L	mgO2/L
-15.66														
-1.63					2210	3020	185	695			2110	0.02	2280	262.5
-1.49	424	404												
0.73				46	2150	2940	180	675				43.7		
2.74											2200	43.2	2330	
8.73				44	2350	3200	197	735			2250	38.5	2350	
23.63			2295	<20	2270	3050	186	710	2030	1870	2220	0.002	2380	326
25.60				<20	2280	3050	187	700				12.8		
26.11											2240	9.6	2400	
27.61											2440	2.3	2420	488
28.56				<20	2275	3020	187	700						
30.06											2310	14.2	2400	
32.08			2250	<20	2365	2365	191	715	2060	1840		2.5		
32.58											2190	0.74	2370	
46.61											2200		2400	348
48.51					2365							10.4		
49.01											2180	7.1	2420	
50.01			2290	<20	2380	3120	192	715	2130	1875		0.66		
52.79	467	433												
Average	446	419	2278	45	2294	2971	188	706	2073	1862	2234	13	2375	356
Stdev	30.4	20.5	24.7	1.4	78.7	256.4	5.1	17.6	51.3	18.9	89.0	16.2	44.3	95.1
Samples	2	2	3	2	9	8	8	8	3	3	10	14	10	4

Table 15: Nitrite measurements during the calibration experiment. The horizontal lines indicate the pulse additions

Time	Measurement 1				Measurement 2				Used
	Analysis time	Dilu-tion	TNN	Test kit	Analysis time	Dilu-tion	TNN	Test kit	TNN
	h after samp-ling	1:	mgN/L		h after samp-ling	1:	mgN/L		mgN/L
-1.63		1	0.039	LCK 342		1	0.017	LCK 341	0.017
0.23		11	43.78	LCK342					43.78
0.73		11	43.01	LCK342	26.4	20	44.4	LCK 342	43.705
1.26		10	43.3	LCK342					43.3
2.74	24.3	20	43.2	LCK 342					43.2
4.78	24.3	10	39.8	LCK 342					39.8
6.75	22.3	20	39.2	LCK 342					39.2
8.73	0.2	10	37.5	LCK 342	18.4	20	39.4		38.45
21.35	5.7	20	5.58	LCK 341					5.58
21.83	5.3	20	3.32	LCK 341					3.32
22.33	4.8	20	1.34	LCK 341					1.34
23.63	3.5	20	0.0016	LCK 341					0.0016
24.11	3.0	20	20	LCK 341		20	18.34	LCK 342	19.17
24.61	2.5	20	17.6	LCK 341		20	16.48	LCK 342	17.04
25.11	2.0	20	15.2	LCK 341		20	14.58	LCK 342	14.89
25.60	26.2	14.3	12.84	LCK342					12.84
26.11	24.5	20	9.64	LCK 342					9.64
26.61	25.2	20	7.54	LCK 341					7.54
27.11	24.7	20	5.1	LCK 341					5.1
27.61	23.0	20	2.28	LCK 341					2.28
28.06	23.8	20	negative	LCK 342	0.3	20	0.66	LCK341	0.66
28.56	23.3	20	negative	LCK 342					
29.06	22.8	20	19.6	LCK 342					19.6
29.56	22.3	20	16.58	LCK 342					16.58
30.06	20.5	20	14.16	LCK 342					14.16
30.56	21.3	25	11.35	LCK 341					11.35
31.06	20.8	20	8.44	LCK 341					8.44
31.58	20.3	20	5.4	LCK 341					5.4
32.08	19.8	20	2.46	LCK 341					2.46
32.58	19.7	20	0.74	LCK 341					0.74
47.01	5.3	20	19.22	LCK 342					19.22
47.51	4.7	20	16.18	LCK 342					16.18
48.01	4.2	25	13.425	LCK 341					13.425
48.51	3.8	20	10.38	LCK 341					10.38
49.01	1.6	20	7.12	LCK 341					7.12
49.51	2.7	20	4.08	LCK 341					4.08
50.01	2.3	20	0.66	LCK 341					0.66
	red: below / above measuring range of test kit				orange: matrix effects not negligible				green: only second measurement

A.6.2. Validation experiment

Table 16 shows the measurements during the validation experiment.

Table 16: Measurements during the validation experiment

Time	Biomass		Dr. Lange				Ion chromatography			
	TSS	VSS	COD_{diss}	TAN	TNN	NO_3-N	NO_3-N	Cl^-	PO_4^{3-}	SO_4^{2-}
	mg/L	mg/L	mg/L	mgN/L	mgN/L	mgN/L	mgN/L	mg/L	mgP/L	mgS/L
-0.02			330	2180		2360	2370	3190	190	720
0.50					3.29					
1.00					7.65					
1.51					8.93					
2.01					9.15					
2.50					8.43					
3.00					6.9					
3.67					4.2					
4.17					1.61					
21.05	664	614								

A.7. Calibration

A.7.1. Initial sensitivity analysis

An initial sensitivity analysis using $X_{NOB}(0)$=0.012 gCOD/L was performed. Figure 15 shows the sensitivity analyses for the phase when NOB were strongly inhibited (hours 0-17), the for each single pulse and for all pulses. Some curves or data points are missing due to numerical problems in Matlab.
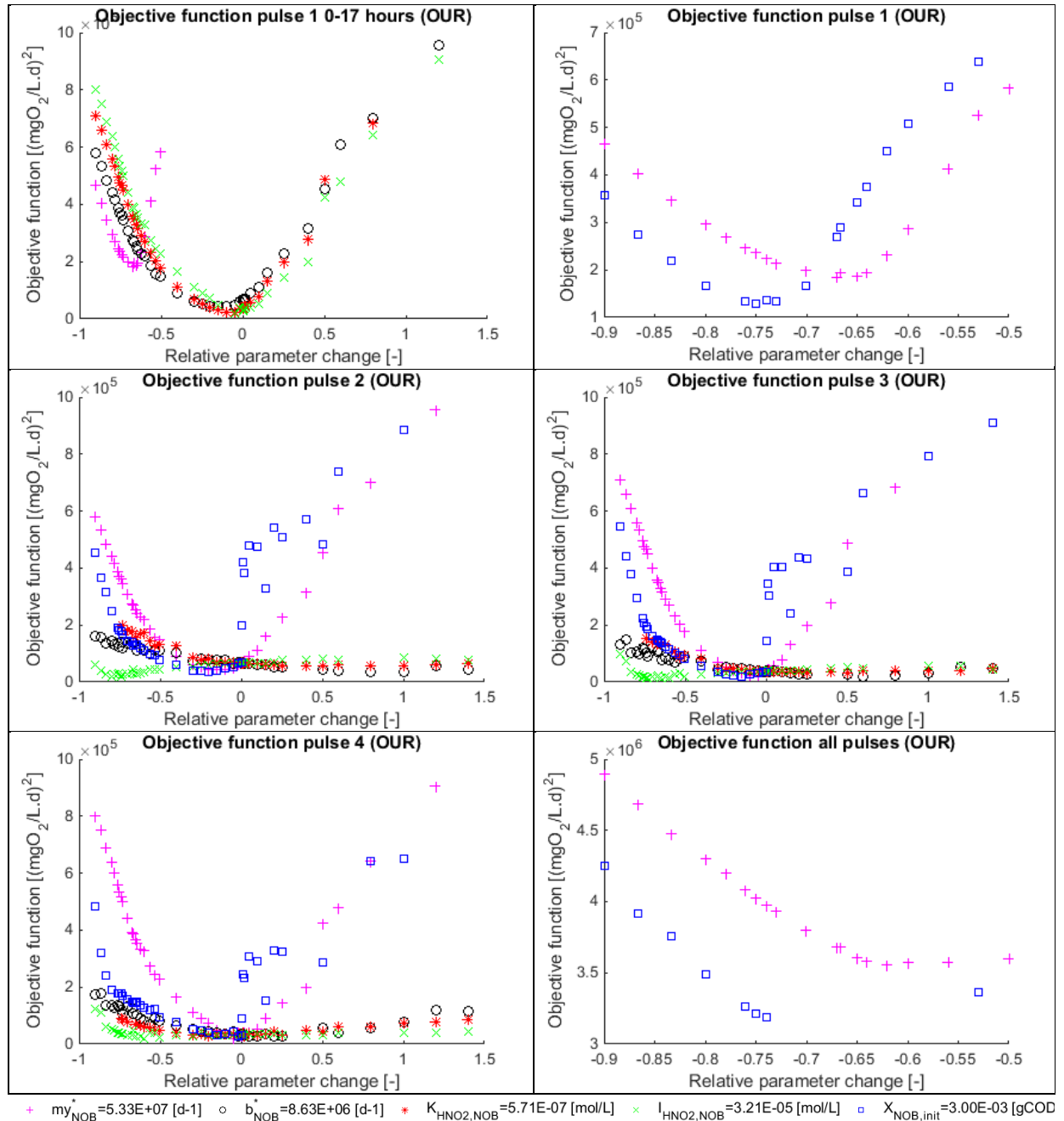

Figure 15: Initial sensitivity analysis with an initial biomass concentration of $X_{NOB}(0)$=0.012 gCOD/L. The step for $X_{NOB,init}$ above 0 is due to an error in the Matlab code (corrected for subsequent simulations). The objective values actually correspond to double the relative parameter change than shown (e.g., the objective function at 0.5 is actually the value of a relative parameter change of 1).

A.7.2. Estimation of initial biomass concentration from activity peaks

The uncertainty of the initial NOB biomass concentration was estimated from the ratios of each measured OUR peak relative to the first OUR peak. A maximal measurement deviation of 4% was assumed for each peak (uncertainty of single measurement, c.p. Figure 22, appendix A.7.5). It was not chosen higher since only the ratios of the peaks, not their absolute values are needed (see section 2.3.6). In order to estimate the initial biomass concentration, the following objective function was minimized, $OUR_{TNN,mod}(i)$ being the modelled, non-endogenous OUR peak i and $OUR_{TNN,obs}(i)$ the measured one:

Objective function = $\Sigma[OUR_{TNN,mod}(i)/OUR_{TNN,mod}(1)-OUR_{TNN,obs}(i)/OUR_{TNN,obs}(1)]^2$

The OUR measurements with their uncertainty range and the ratios of them and the needed ratios for the average, the lower and the upper limit are given in Table 17. The minimum of each objective function is displayed in Figure 16 unterhalb. The optimal values of 0.004, 0.005 and 0.065 mgCOD/L as the lower, the expected and the upper estimate, respectively, are highlighted in red. The values and the intermediate results can be found in Table 18 on the next page.

Table 17: OUR peaks with their uncertainty range and the ratios used to calculate the expected (column 4), the minimal (column 5) and the maximal (column 6) of the biomass concentration

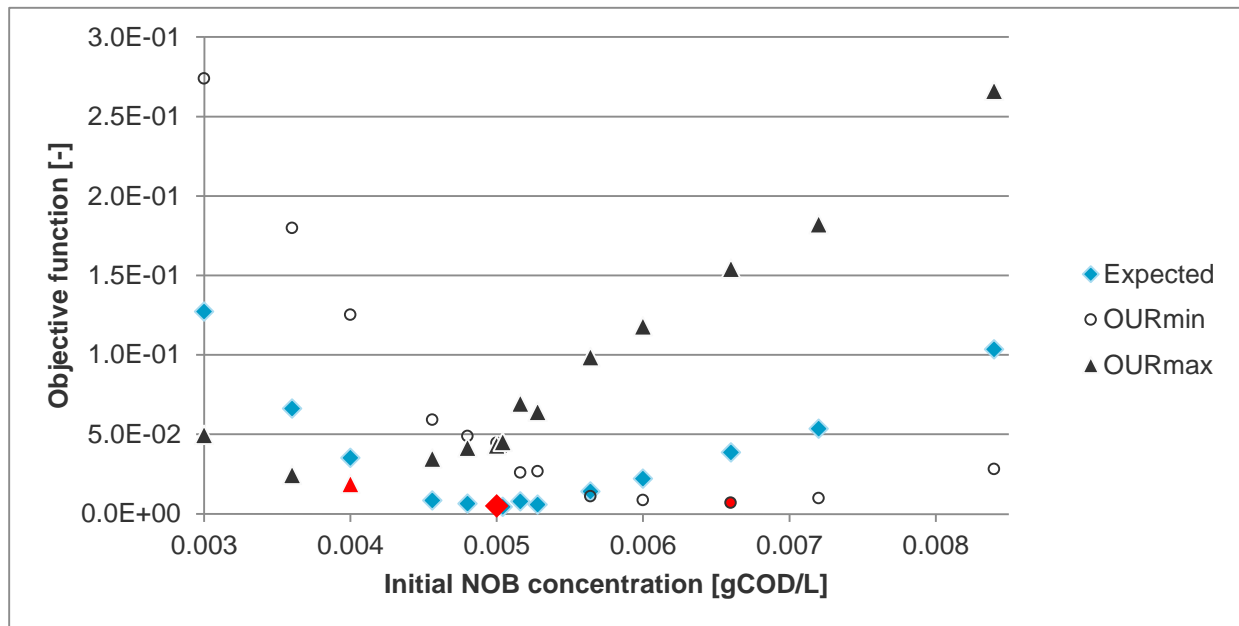|	OUR_{TNN}	$OUR_{TNN,min}$	$OUR_{TNN,max}$	$OUR_{TNN}(i)/$ $OUR_{TNN}(1)$	$OUR_{TNN,min}(i)/$ $OUR_{TNN,max}(1)$	$OUR_{TNN,max}(i)/$ $OUR_{TNN,min}(1)$
	$mgO_2/L.d$	$mgO_2/L.d$	$mgO_2/L.d$	-	-	-
Peak 1	130±5.2	125	135	1.00±0.08	0.92	1.08
Peak 2	156±6.2	149	162	1.20±0.10	1.10	1.30
Peak 3	172±6.9	165	179	1.32±0.11	1.22	1.43
Peak 4	179±7.2	172	187	1.38±0.11	1.27	1.49

Figure 16: Estimation of the initial biomass concentration from the OUR peaks taking into account the uncertainty of the OUR measurements. As objective function, i.e.. The optima are indicated in read.

Table 18: Modelled peaks at different biomass concentrations as well as ratios and squared residuals, which are summed up to the objective function for the expected, the minimal and the maximal value. The optima are highlighted.

X_0 [10^3 gCOD/L]

	3.0	3.6	4.0	4.6	4.8	5.0	5.0	5.2	5.3	5.6	6.0	6.6	7.2	8.4
$OUR_{TNN,mod}$ [mgO_2/L.d]														
Peak 1	55.8	62.6	67.5	71.8	74.6	76.2	77.1	78.0	79.1	82.7	89.8	96.3	100.9	115.9
Peak 2	69.4	76.0	80.8	82.8	85.3	87.3	88.3	86.6	89.0	91.4	97.6	103.7	106.7	118.8
Peak 3	84.2	91.5	96.0	97.6	100.4	102.0	103.1	101.8	103.2	105.3	112.8	118.0	121.9	133.4
Peak 4	93.7	99.8	103.8	104.3	107.0	108.6	109.3	108.1	110.0	109.3	117.3	121.3	124.6	135.5
$OUR_{TNN}(i)/OUR_{TNN}(1)$ [-]														
Peak 1	1.00	1.00	1.00	1.00	1.00	1.00	1.00	1.00	1.00	1.00	1.00	1.00	1.00	1.00
Peak 2	1.25	1.22	1.20	1.15	1.14	1.15	1.14	1.11	1.12	1.11	1.09	1.08	1.06	1.03
Peak 3	1.51	1.46	1.42	1.36	1.35	1.34	1.34	1.31	1.30	1.27	1.26	1.22	1.21	1.15
Peak 4	1.68	1.60	1.54	1.45	1.43	1.43	1.42	1.39	1.39	1.32	1.31	1.26	1.23	1.17
Squared residuals (expected value) [[$OUR_{TNN,mod}(i)/OUR_{TNN,mod}(1)$] − [($OUR_{TNN,obs}(i)/OUR_{TNN,obs}(1)$)]]^2 [$1*10^3$]														
Peak 1	0.00	0.00	0.00	0.00	0.00	0.00	0.00	0.00	0.00	0.00	0.00	0.00	0.00	0.00
Peak 2	2.36	0.36	0.00	1.87	2.85	2.52	2.70	7.37	5.22	8.32	12.06	14.42	19.35	29.43
Peak 3	34.81	19.35	9.86	1.31	0.54	0.26	0.19	0.30	0.36	2.43	4.49	9.62	13.20	29.59
Peak 4	90.07	46.46	25.22	5.21	3.01	2.10	1.40	0.05	0.10	3.34	5.45	14.56	21.02	44.42
Sum	127.2	66.2	35.1	8.4	6.4	4.9	4.3	7.7	5.7	14.1	22.0	38.6	53.6	103.4
Squared residuals (minimum) [[$OUR_{TNN,mod}(i)/OUR_{TNN,mod}(1)$] − [($OUR_{TNN,obs,min}(i)/OUR_{TNN,obs,max}(1)$)]]^2 [$1*10^3$]														
Peak 1	5.92	5.92	5.92	5.92	5.92	5.92	5.92	5.92	5.92	5.92	5.92	5.92	5.92	5.92
Peak 2	19.79	12.31	8.69	2.38	1.50	1.75	1.60	0.04	0.39	0.00	0.32	0.79	2.21	6.32
Peak 3	83.15	58.02	40.43	19.03	15.62	13.89	13.37	7.15	6.85	2.76	1.21	0.01	0.17	4.94
Peak 4	165.05	103.48	70.20	31.79	25.91	23.11	20.60	12.74	13.50	2.34	1.05	0.21	1.51	10.95
Sum	273.9	179.7	125.2	59.1	48.9	44.7	41.5	25.8	26.7	11.0	8.5	6.9	9.8	28.1
Squared residuals (maximum) [[$OUR_{TNN,mod}(i)/OUR_{TNN,mod}(1)$] − [($OUR_{TNN,obs,max}(i)/OUR_{TNN,obs,min}(1)$)]]^2 [$1*10^3$]														
Peak 1	6.94	6.94	6.94	6.94	6.94	6.94	6.94	6.94	6.94	6.94	6.94	6.94	6.94	6.94
Peak 2	2.61	6.53	9.71	20.45	23.43	22.47	23.01	34.44	29.57	36.45	43.91	48.30	57.03	73.58
Peak 3	5.83	0.83	0.12	5.49	7.58	8.87	9.29	16.25	16.70	25.45	31.43	43.39	50.69	79.68
Peak 4	34.27	10.11	1.92	1.83	3.62	4.78	6.02	11.72	11.01	29.84	35.64	55.54	67.59	106.12
Sum	49.7	24.4	18.7	34.7	41.6	43.1	45.3	69.4	64.2	98.7	117.9	154.2	182.3	266.3

A.7.3. Sensitivity analysis with estimated biomass concentration

The estimated initial biomass concentration of $X_{NOB}(0)$=0.005 gCOD/L was used for another sensitivity analysis (Figure 17). A sensitivity analysis for the lower range ($X_{NOB}(0)$=0.004 gCOD/L) is given in Figure 18 on the next page, for the upper range of $X_{NOB}(0)$=0.0065 gCOD/L in Figure 19 on the page after.
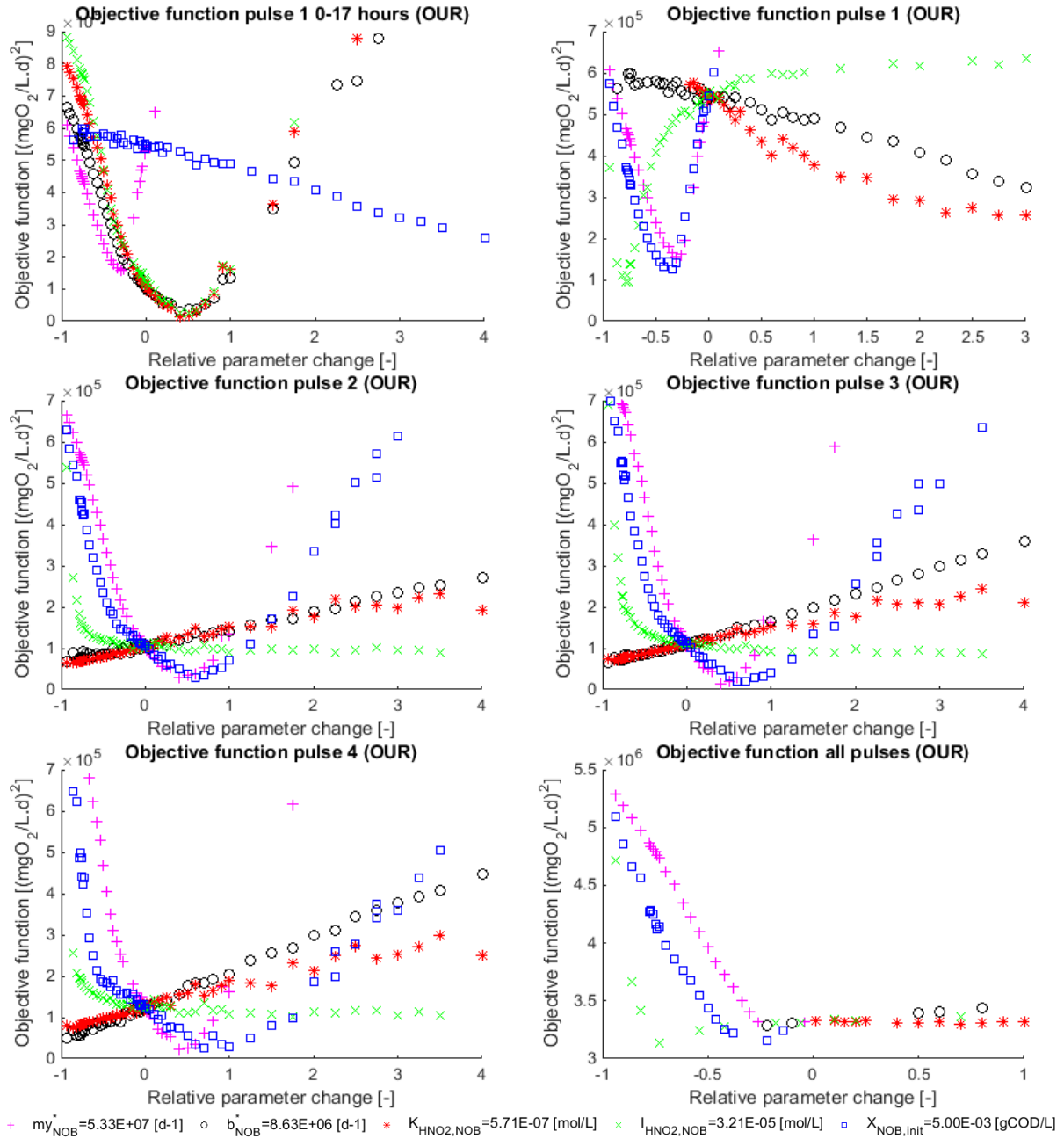

Figure 17: Sensitivity analysis for the estimated initial biomass concentration of $X_{NOB}(0)$=0.005 gCOD/L. Only the range with high sensitivities of some parameters is shown.
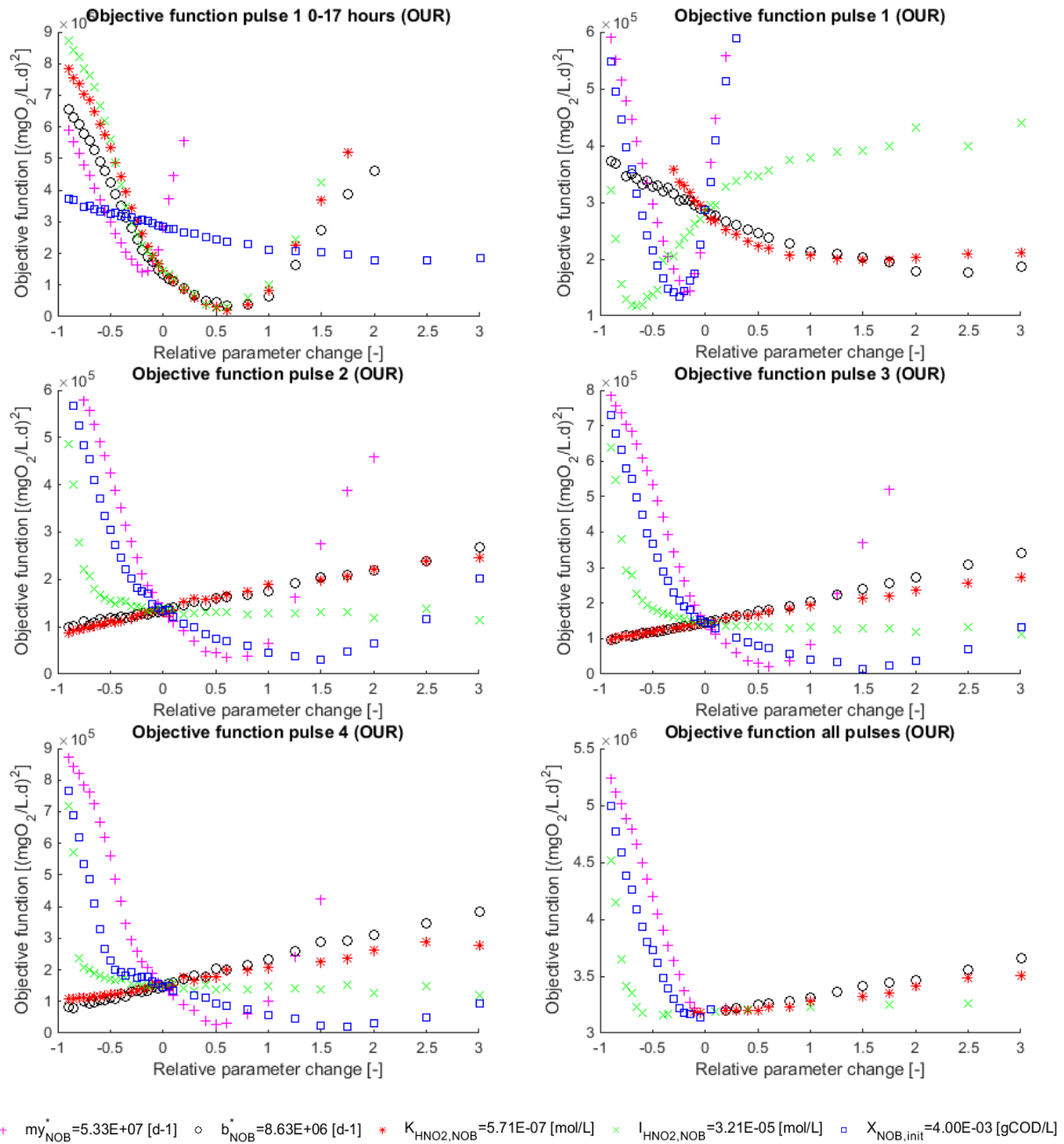
Figure 18: Sensitivity analysis for the low range of the estimated initial biomass concentration ($X_{NOB}(0)$=0.004) gCOD/L. Only the range with high sensitivities of some parameters are shown.
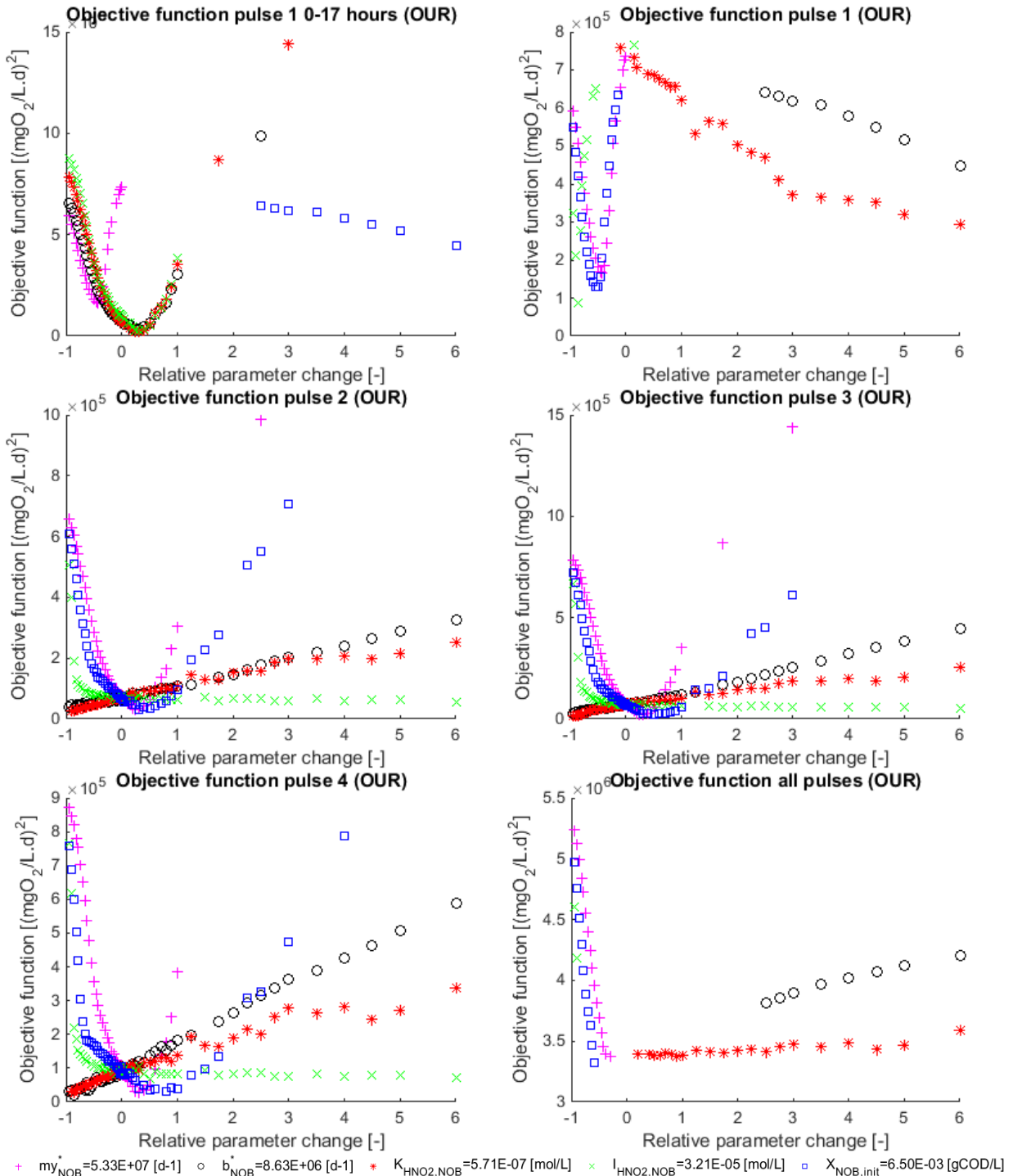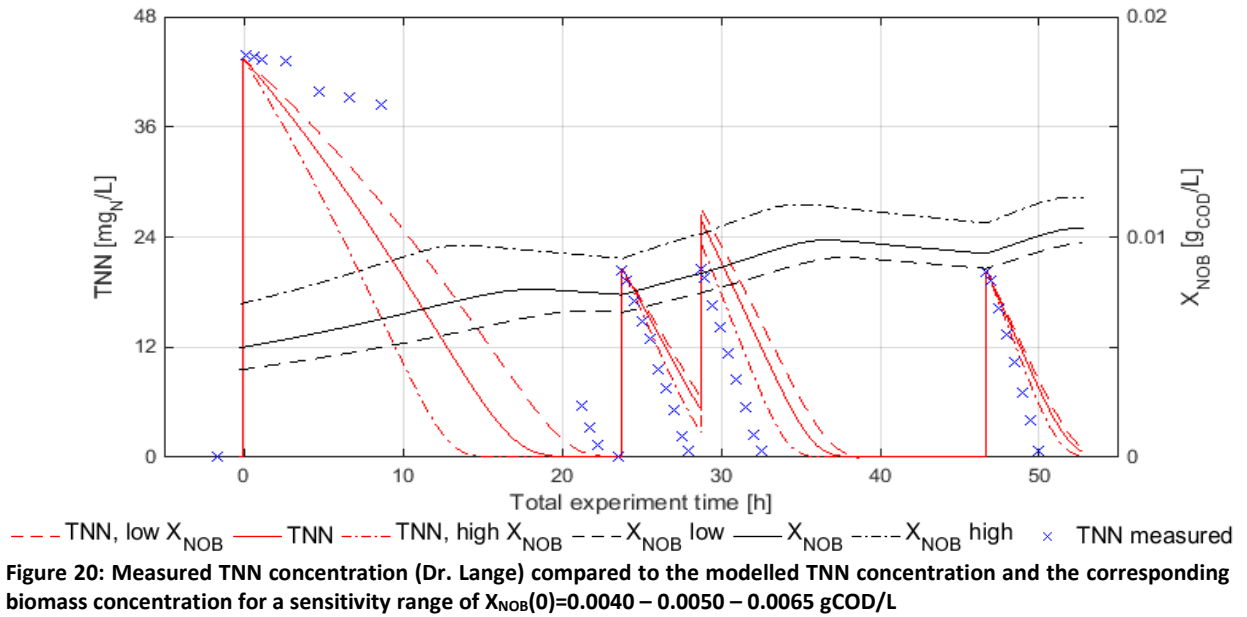
Figure 19: Sensitivity analysis for the high range of the estimated initial biomass concentration ($X_{NOB}(0)$=0.0065) gCOD/L.

A.7.4. Additional graphs with the estimated biomass concentration

Figure 20 shows the development of the TNN concentration for the range of biomass concentrations. The slope of TNN degradation is steeper than observed at large concentrations (beginning of the experiment) but too gentle at lower concentrations (pulses 2-4). The graph additionally shows that there is growth of NOB after pulse additions and decay after almost complete degradation (below 0.5 mgNO$_2$-N/L) of pulse 1 and pulse 3. The activity peaks of NOB (c.p. Figure 5) occur at a concentration of 15 mgNO$_2$-N/L.

Figure 20: Measured TNN concentration (Dr. Lange) compared to the modelled TNN concentration and the corresponding biomass concentration for a sensitivity range of X$_{NOB}$(0)=0.0040 – 0.0050 – 0.0065 gCOD/L
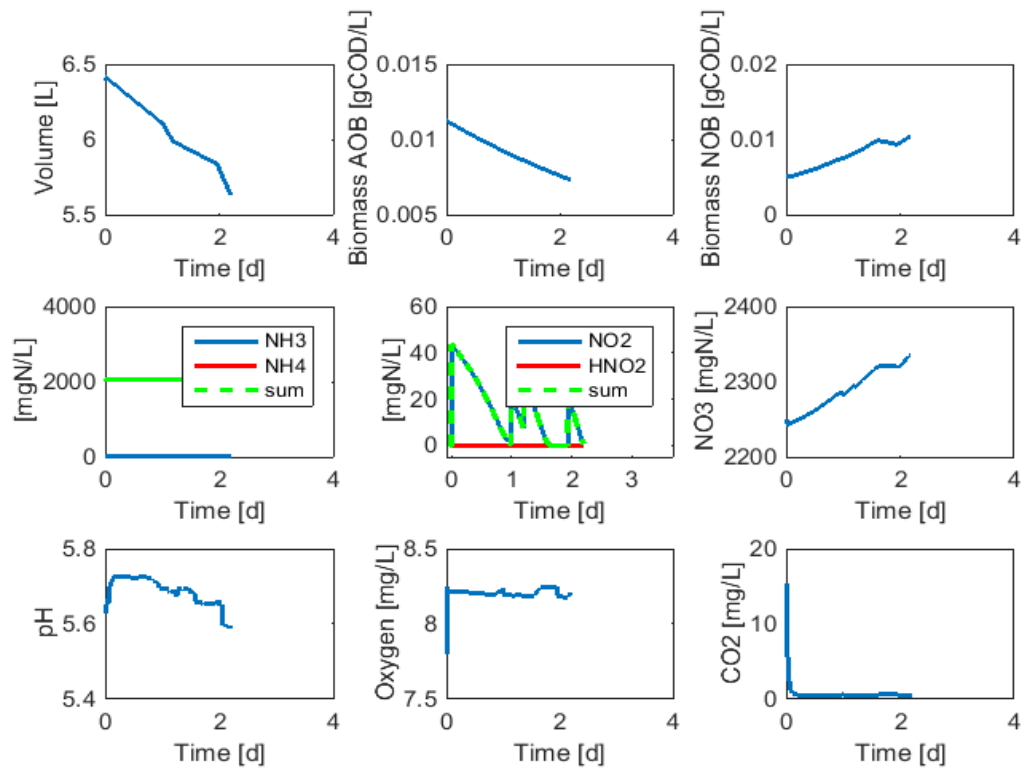
Figure 21: Development of the different variables for the calibration experiment with the estimated initial biomass concentration $X_{NOB}(0)$ = 0.005 gCOD/L.

A.7.5. Estimation of $K_{I,HNO2,NOB}$ from activity peaks

In order to estimate the uncertainty of the $K_{I,HNO2,NOB}$ estimate, the HNO_2 concentration at maximal activity must be known. The most uncertain factors on TNN concentration at the activity peak are assumed to be the time of the activity peak (max. ±8min), the pH measurement (±0.03 units) and the TNN measurements itself (every 30 minutes, max. ±5% each measurement). The acid-base equilibrium of HNO_2 and NO_2^- (pK_a = 3.25) is not considered since the value is used both as a parameter of the nitrification model and for estimation of $K_{I,HNO2,NOB}$.

As an example of how the time uncertainty is estimated, the OUR measurements of the peak with the largest fluctuations (peak 4) are shown in Figure 22.
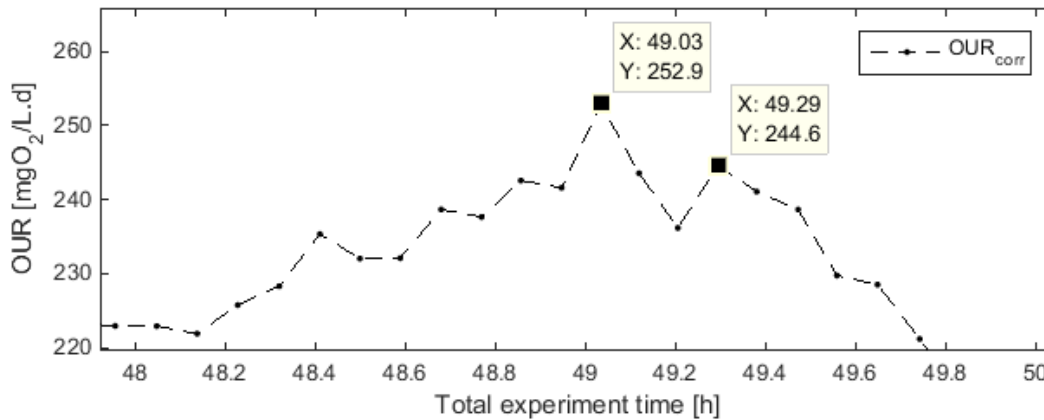

Figure 22: Corrected OUR at the time of peak 4. The first datatip is the measured maximal OUR, the second data tip the one used for calibration (2nd largest value). The time between the two values (0.26h) is assumed to represent the maximal uncertainty range, which is therefore assumed 8min (0.13h). This corresponds to about three subsequent OUR measurements.

The results for the uncertainty of TNN concentration at the peak due to uncertainty of the time of peak occurrence is shown in Table 19.

Table 19: Uncertainty of TNN concentration at activity peak due to time uncertainty: calculated as maximal nitratation rate ($r_{N,max}$) times the time uncertainty of peak occurrence (dt = 8min)

	$r_{N,max}$ mgN/L.d	TNN uncertainty range (dt=8min) mgTNN/L
Pulse 1	114	0.63
Pulse 2	136	0.76
Pulse 3	150	0.84
Pulse 4	157	0.87
Pulse 4 (max)	164	0.91
Average (without max. pulse 4)	139	0.77

For assessment of the uncertainty of the $K_{I,HNO2,NOB}$ estimate, the average time uncertainty is used (neglecting the maximal value of pulse 4, c.p. table oben). This value is then added to the uncertainty of the Lange measurement and the pH measurement in order to obtain the total uncertainty of the HNO_2 concentration of a single OUR peak (Table 20). The table shows that the peak time contributes about half of the uncertainty. The HNO_2 is calculated for pH 5.65 and an activity coefficient of 0.71 due to 22 mg/L salinity.

Since there are multiple measurements (4 peaks), the uncertainty can further be reduced. For this purpose, the previously defined uncertainty is assumed to be double the standard deviation of a normal distribution ($2 \cdot \sigma_x$), which allows dividing the uncertainty range by $\sqrt{n-1}$ (Table 20).

Table 20: Uncertainty of the most important factors that influence TNN and HNO$_2$ concentration at S$_{TNN}$ = 6 mgN/L (S$_{HNO2}$ = 1.22·10^{-6} mol/L). The total uncertainty of 4 measurements is used for estimating K$_{I,HNO2,NO}$. Valid at pH 5.65 and a salinity of 22mg/L.

Variable	TNN	HNO$_2$		Remarks
			±	
	mgTNN/L	molHNO$_2$/L	(%)	
Uncertainty of individual variables				
Lange measurement (±5%)	6.0±0.3	6.1E-08	5%	
pH measurement (±0.03)	6.0±0.0	8.1E-08	7%	
Peak time (±8min)	6.0±0.8	1.6E-07	13%	
Total uncertainty				
				Assumed 2·σ of a normal distri-
Single measurement	1.07	3.0E-07	25%	bution
4 measurments (2·σ)	0.62	1.7E-07	14%	Divided by $\sqrt{n-1}$

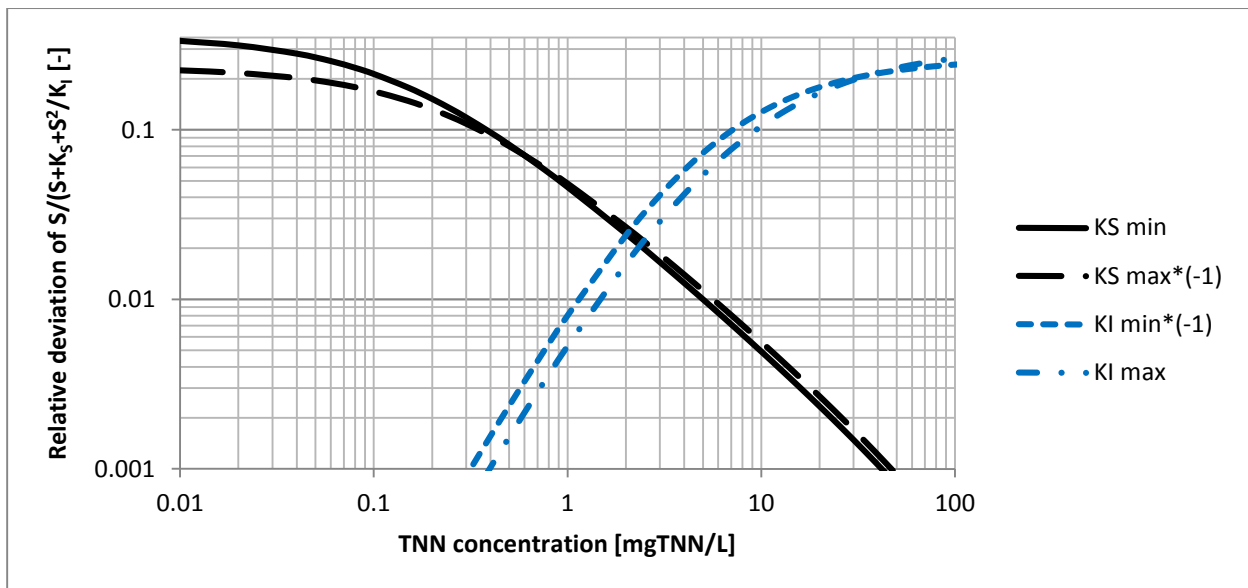### A.7.6. Sensitivity range of estimated K$_{I,HNO2,NOB}$

Figure 23: Relative deviation of the affinity-inhibition term from the average (shown in Figure 8 on the left) for both parameters as a function of TNN concentration (pH 5.65)

The simulation of the experiment with the parameter estimates and their range are shown in the following graphs. Figure 24 shows the course of the TNN and of the NOB biomass concentration, Figure 25 the course of the OUR. For OUR and TNN, the measurements are given for comparison. The initial biomass concentration is taken from the calibration in section 3.2.
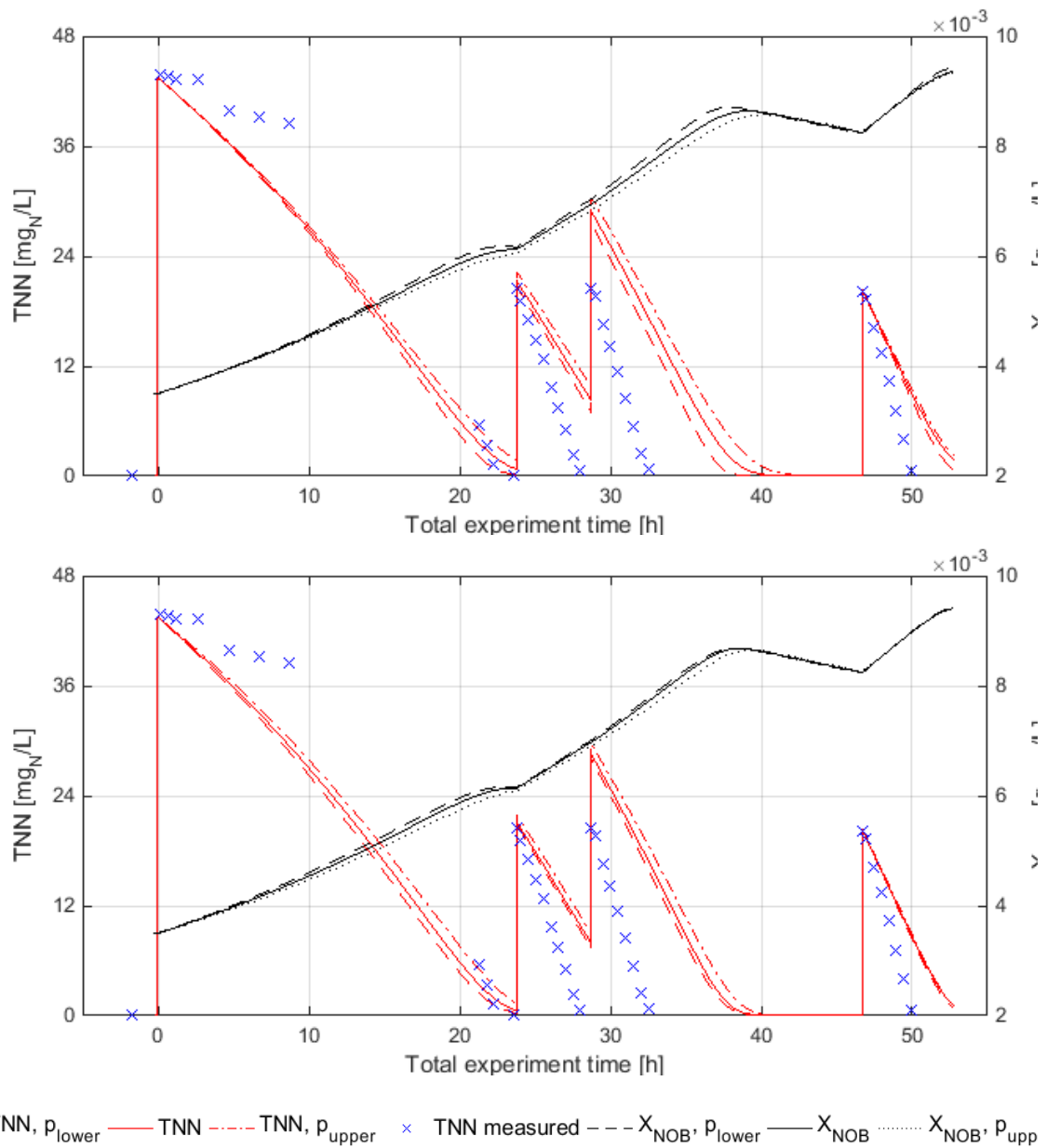
**Figure 24: Sensitivity range of $X_{NOB}(0)$ and TNN concentration with the parameters estimated from the activity peaks –
Figure above: Sensitivity range for $K_{S,HNO2,NOB}$ = 3.0 – 4.1 – 5.3E-08 molHNO₂/L using $K_{I,HNO2,NOB}$ = 3.21E-05 molHNO₂/L
(original value). – Figure below: Sensitivity range for $K_{I,HNO2,NOB}$ = 1.7 – 2.3 – 3.0E-06 molHNO₂/L using $K_{S,HNO2,NOB}$ = 5.7E-
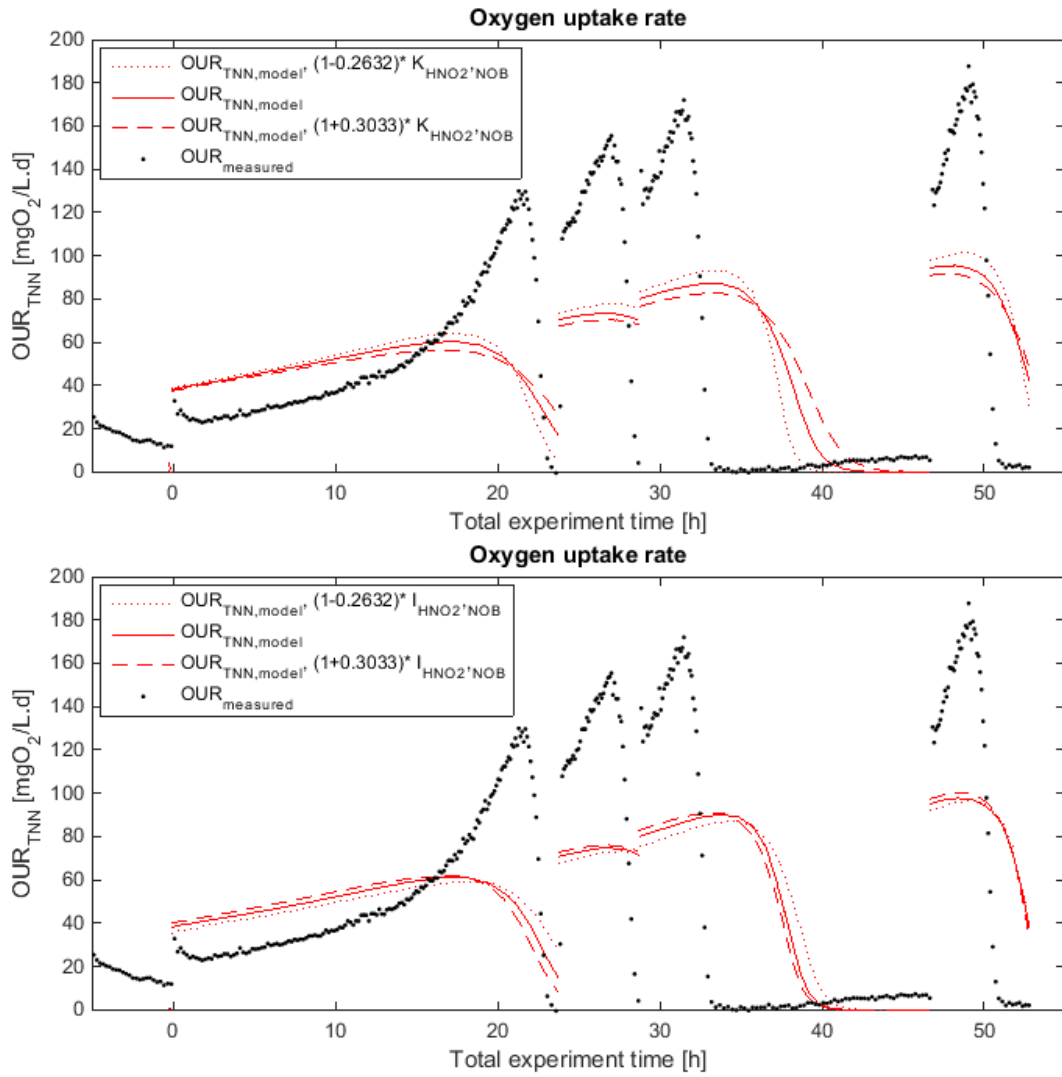07 molHNO₂/L (original value).**

Figure 25: Sensitivity range of OUR with the parameters estimated from the activity peaks. − Figure above: Sensitivity range for $K_{S,HNO2,NOB}$ = 3.0 − 4.1 − 5.3E-08 molHNO₂/L using the original $K_{I,HNO2,NOB}$ = 3.21E-05 molHNO₂/L. − Figure below: Sensitivity range for $K_{I,HNO2,NOB}$ = 1.7 − 2.3 − 3.0E-06 molHNO₂/L using the original $K_{S,HNO2,NOB}$ = 5.7E-07 molHNO₂/L.

A.7.7. Relative activity after pulse additions

Table 21: First activity measurements after pulse additions 2 and 3

Pulse addition	First activity measurement after pulse addition			
No.	Experiment time	Time after pulse addition	r	Concentration
	h	min	mgN/L.d	mgTNN/L
Pulse 2	23.99	8.4	94	19.9±0.5
Pulse 3	28.96	9.6	108	19.8±0.5

Table 22: First activity measurements after pulse additions 2 and 3 (r) relative to the maximal activity measured at the last peak ($r_{max,last}$) and the next peak ($r_{max,next}$). All activities are already reduced by the endogenous respiration rate (53.9 and 57.1 mgO_2/L.d for pulse 2 and 3, respectively). The duration between the measurement and the peaks are also given.

Pulse	Measurement	Relative to last peak			Relative to next peak		
No.	r	Duration since last peak	$r_{max, last}$	$r/r_{max,last}$	Duration until next peak	$r_{max,next}$	$r/r_{max,next}$
	mgO_2/L.d	h	mgO_2/L.d	-	h	mgO_2/L.d	-
2	108	2.7	130.0	0.83	3.0	155.5	0.69
3	124	1.9	155.5	0.80	2.5	171.9	0.72

A.8. Data CDs

Data CD1

- Directory of the Master thesis including the calculations and the report

Data CD2

- Additional calibration results